LECTURE 5:
Development of mechanistic empirical design methods

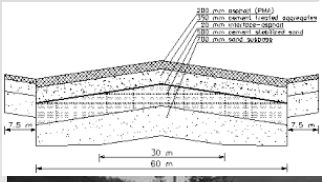

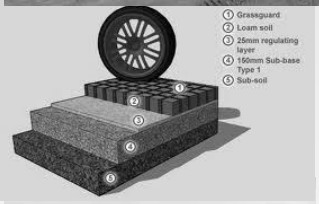

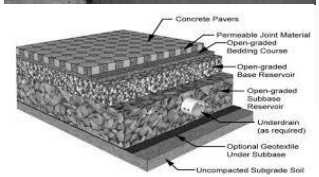

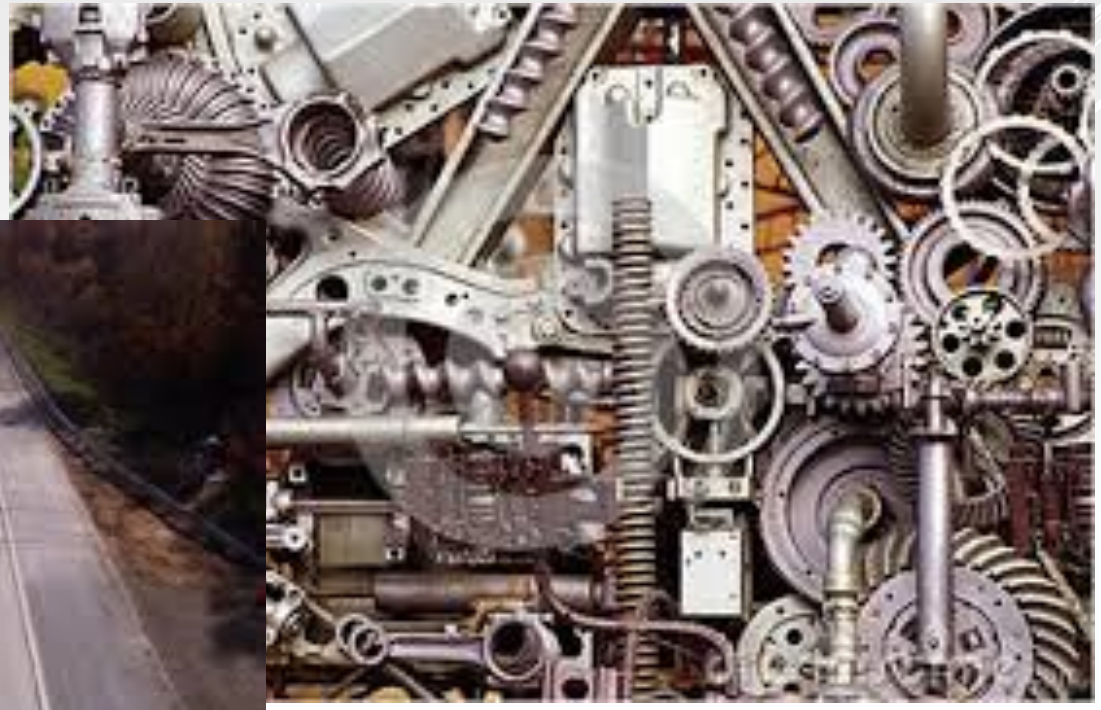

5.1 Introduction

- Although the AASHTO design method was a major step forward it still had the drawback of being highly empirical. The method in fact is nothing less than a set of regression equations which are valid for the specific conditions (climate, traffic, materials etc.) of the Road Test.

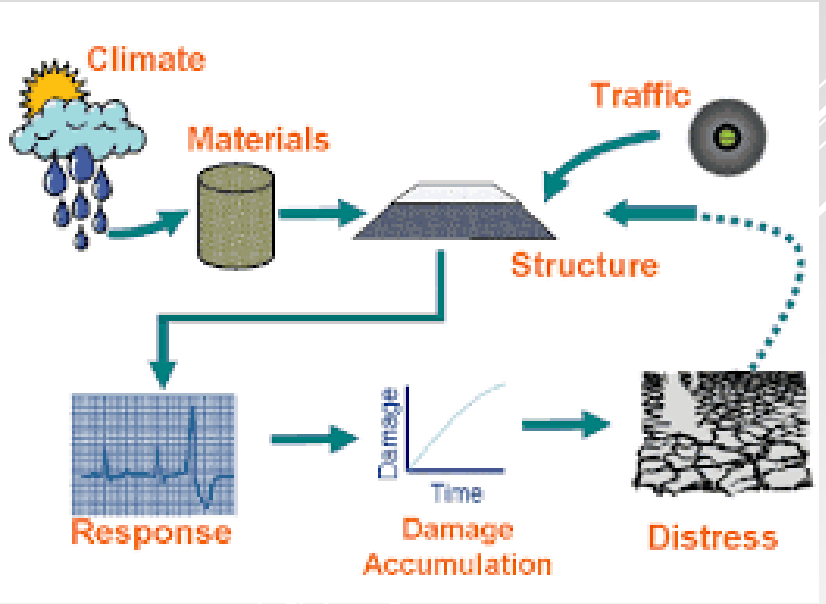

- This implies that it is a bit risky to use the method in tropical countries where the conditions are completely different. Fortunately, road constructions are forgiving structures implying that the method at least results in an initial design that can be refined to meet local conditions.

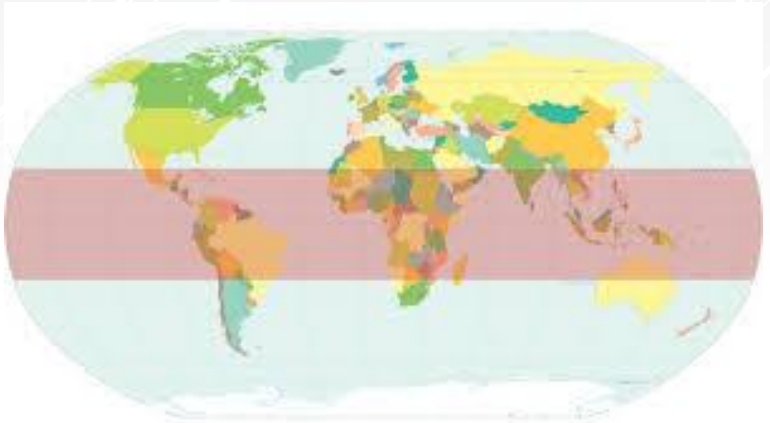

- The fact that the AASHTO method cannot be directly used for conditions for which it hasn't been developed became very apparent when attempts were made to use it in developing countries.
- The main problem was the PSI concept; it appeared e.g. that a pavement in the developed world with a low PSI implying that immediate maintenance was needed, was still a pavement with an acceptable quality in developing countries.
- This clearly indicated the need to have performance criteria and design methods that fit the needs and circumstances in developing countries.
- All this resulted in the development of the Highway Design Model, a design system that is fully suited for those conditions. It is however beyond the scope of these lecture notes to discuss this model in detail.

- Another problem with the Guide is that it gives no information why materials and structures behave like they do.

- Furthermore the Guide provides no information with respect to maintenance that is needed from a preservation point of view.

- The PSI value e.g. is strongly dependent on pavement roughness and damage types like cracking and rutting don't seem to have a large influence on the PSI. However control of cracking and rutting is important from a preservation point of view and in order to be able to make estimates on such maintenance needs, knowledge on stresses and strains and strength of materials is essential.

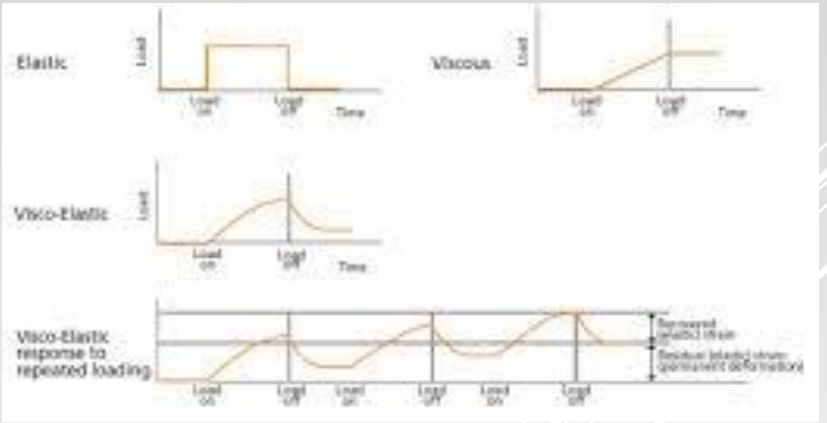

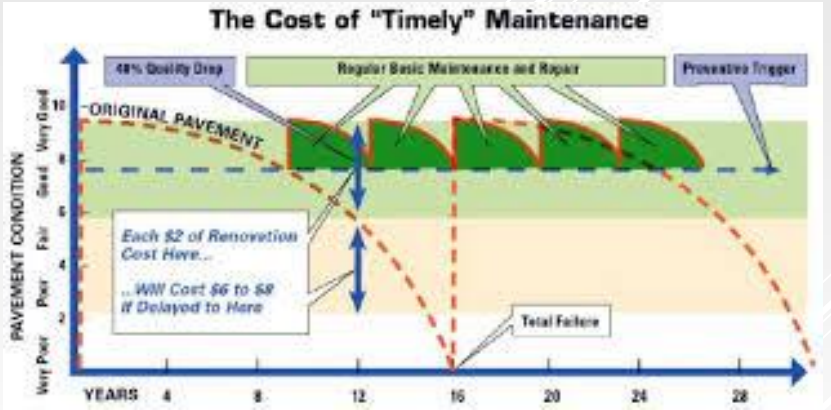

- Furthermore, if such information is not available, then it is almost impossible to evaluate the potential benefits of new types of materials and structures with which no experience has been obtained yet.

- Given these drawbacks, one realized immediately after the Road Test that mechanistic based design tools were needed to support the AASHTO Guide designs. For that reason, much work has been done in the 1960's on the analysis of stresses and strains in layered pavement systems [6,7, 8, 9] and on the characterization of the stiffness, fatigue and permanent deformation characteristics of bound and unbound pavement materials.

- The work done on the analysis of stresses and strains in pavements is all based on early developments by Boussinesq [4] and Burmister [5]. References [10, 11 and 12] are excellent sources with respect to research on pavement modeling and material characterization done in those days and should be on the reading list of any student in pavement engineering. It is remarkable to see that much of the material presented then still is of high value today.

- Since then, much progress has been made and the reader is referred e.g. to the proceedings of the conferences organized by the International Society of Asphalt Pavements, the proceedings of the Association of Asphalt Pavement Technologists, the Research Records of the Transportation Research Board, the proceedings of RILEM conferences on asphalt materials, the proceedings of the International Conferences on the Bearing Capacity of Roads and Airfields and those of many other international conferences to get informed about these developments.

- Given the possibilities we have nowadays with respect to material testing, characterization and modeling, it is possible to model pavements structures as accurate as possible using non linear elasto-visco-plastic models and using advanced finite element techniques that allow damage initiation and progression to be taken into account as well as the effects of stress re-distribution as a result of that.
- Also such methods allow the effects of joints, cracks and other geometry related issues to be taken into account.
- Furthermore these methods also allow to analyze the effects of moving loads which implies that inertia and damping effects can be taken into account.

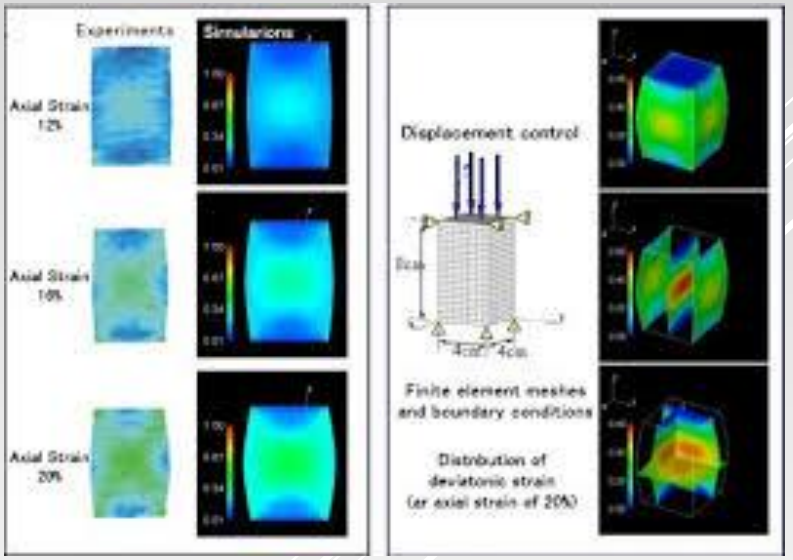

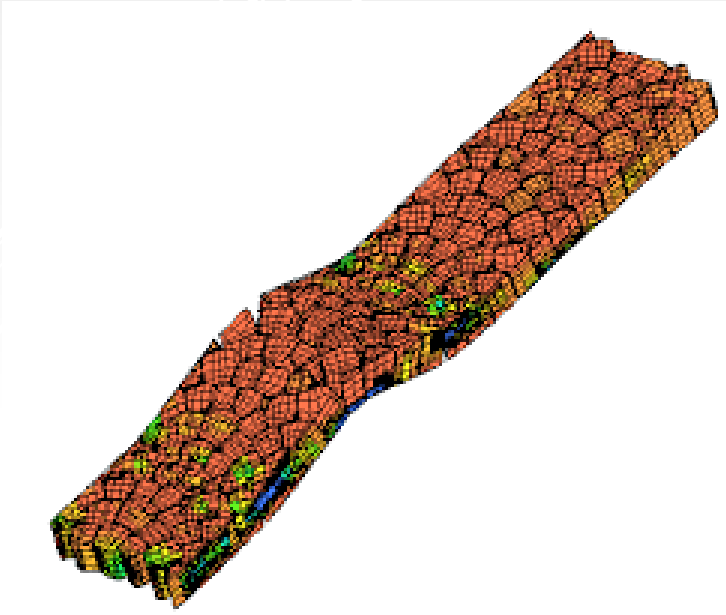

- The question however is to what extent such advanced methods should be used for solving day to day problems. This is a relevant question because advanced pavement design methods involve advanced testing and analyses techniques which require specific hardware and skills.
- Furthermore pavement design is to some extent still an empirical effort because many input parameters cannot be predicted with sufficient accuracy on before hand. Examples of such input parameters are climate, traffic and the quality of the materials as laid and the variation therein.

- All this means that although advanced methods provide a much better insight in why pavements behave like they do, one should realize that even with the most advanced methods one only can achieve a good estimate of e.g. pavement performance. Obtaining an accurate prediction is still impossible.

- Because of this, practice is very much interested in design methods which are, on one hand, based on sound theoretical principles but, on the other hand, are very user friendly and require only a limited amount of testing in order to save money and time.

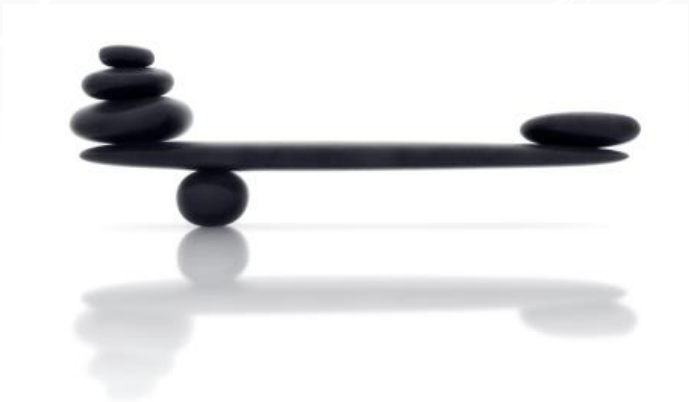

- One should realize that the need to use accurate modeling is influenced to a very large extent by the type of contracts used for road construction projects. In recipe type contracts, the contractor is only responsible for producing and laying mixtures in the way as prescribed by the client.

In this case the contractor is neither responsible for the mixture design nor the design of the pavement structure; these are the responsibilities of the client. This immediately implies that the clients in this case will choose "proven" designs and materials, in other words he will rely on experience, and the contractor has no incentive to spend much effort and resources in advanced material research and pavement design methods.

- If however contractors are made more responsible for what they make, meaning that contractors take over from the authorities the responsibility for the performance of the road over a certain period of time, then they are much more willing to use more advanced ways of material testing and pavement design.

- The purpose of these lecture notes is not to provide an overall picture of existing mechanistic empirical design methods. The goal of these notes is to provide an introduction into pavement design using the analytical methods and material characterization procedures as they are common practice nowadays. This implies that we will concentrate in these notes on the use of multi layer linear elastic systems and the material characterization needed to use these systems.

- Also attention will be paid to how to deal with pavement design in case the main body of the structure consists of unbound materials which exhibit a stress dependent behavior.

- Also the characterization of lime and cement treated layers will be discussed.

5.2 Stresses in a homogeneous half space

- Although pavement structures are layered structures, we start with a discussion of the stresses in a homogeneous half space. Solutions for this were first provided by Boussinesq at the end of the 1800's. Originally Boussinesq developed his equations for a point load but later on the equations were extended for circular wheel loads. The stresses under the center of the wheel load can be calculated using:

$$\sigma_z = p\,[1 - (z^3 / (a^2 + z^2)^{3/2})]$$

$$\sigma_r = \sigma_t = [\{ -(1 + 2v) \} + \{ 2.z.(1 + v) / \sqrt{(a^2 + z^2)} \} - \{ z / \sqrt{(a^2 + z^2)} \}^3] \,.\, p / 2$$

$$w = 2.p.a.(1 - v^2) / E$$

Where:
σ_z = vertical stress,
σ_r = radial stress,
σ_t = tangential stress,
v = Poisson's ratio,
E = elastic modulus,
a = radius of the loading area,
p = contact pressure,
z = depth below the surface.
w = deflection.

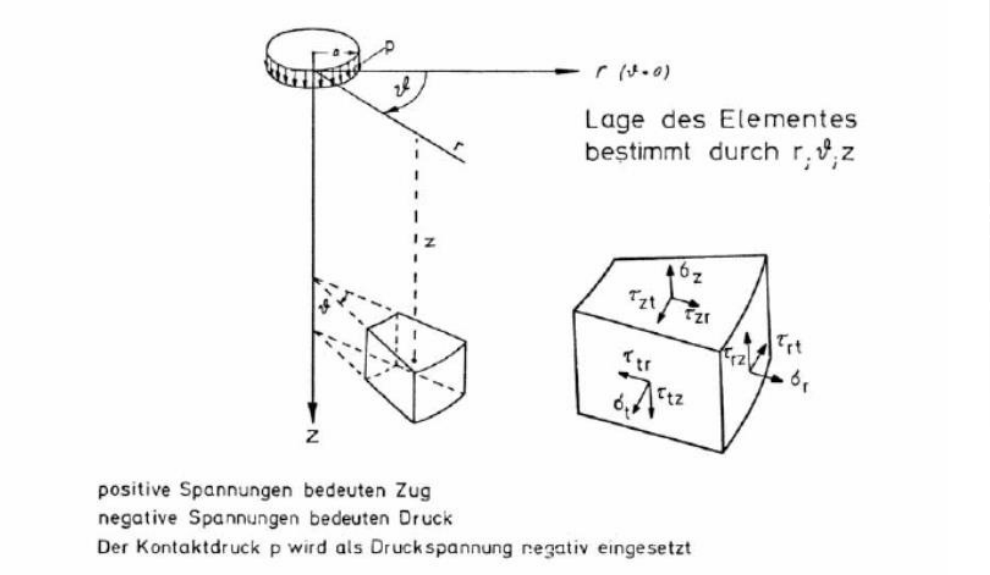

Figure 26: Cartesian and cylindrical coordinate system.

- Please note that the cylindrical coordinate system is used for the formulation of the stresses (see figure 26).
- This is not the place to give the derivations that resulted in the equations given above. The interested reader is referred to [4, 6].
- The Boussinesq equations are useful to estimate stresses in e.g. earth roads where the road structure is built by using the natural available material. One can e.g. derive the Mohr's circles from the calculated stresses and then one can determine whether the stresses that occur are close to the Mohr – Coulomb failure line, implying early failure, or not.

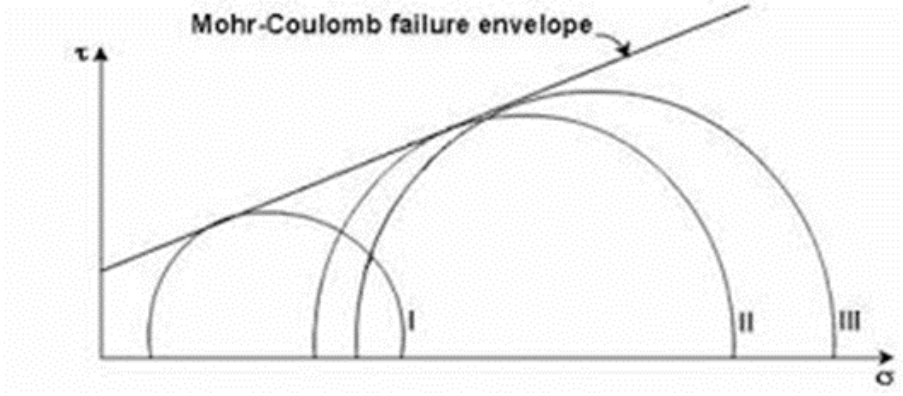

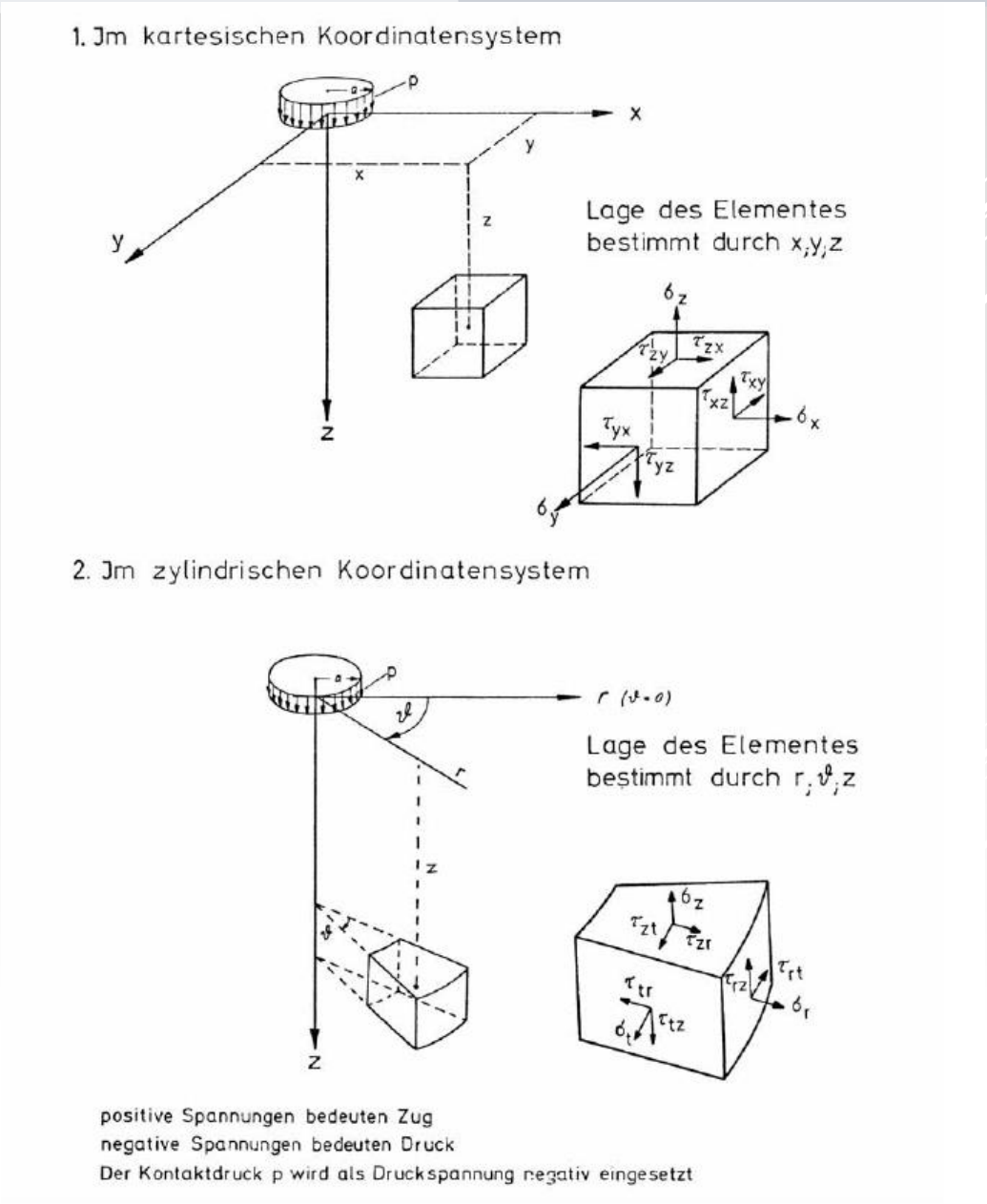

Figure 26: Cartesian and cylindrical coordinate system.

In figure 27 some graphical solutions are provided for the Boussinesq equations.

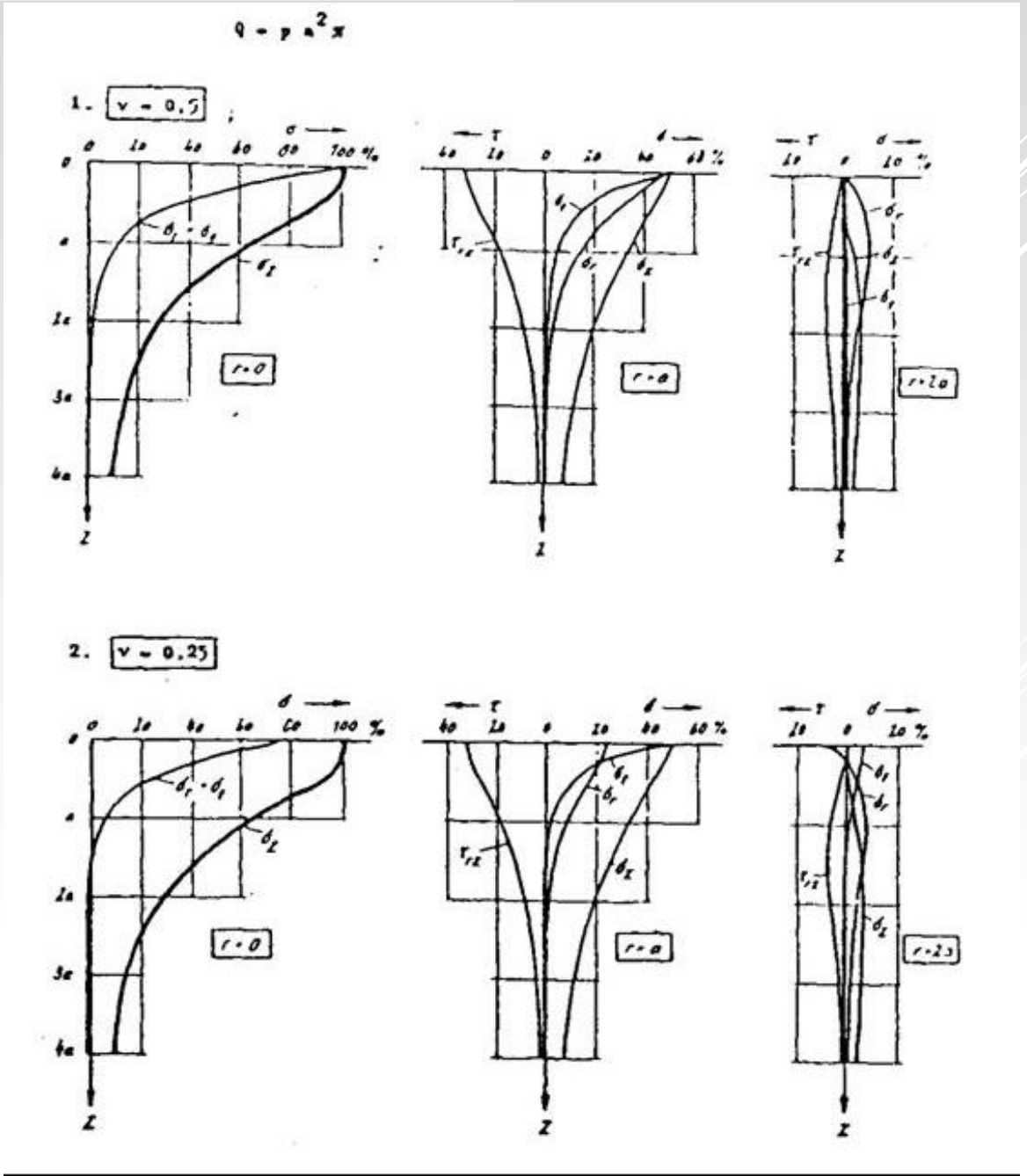

Figure 27: Graphical solutions for Boussinesq's equations.

- Many of these earth roads however are layered systems simply because the top 200 mm or so have different characteristics than the original material simply because of compaction that is applied etc. The higher stiffness of this top layer results in a better spreading of the load. This is schematically shown in figure 28.

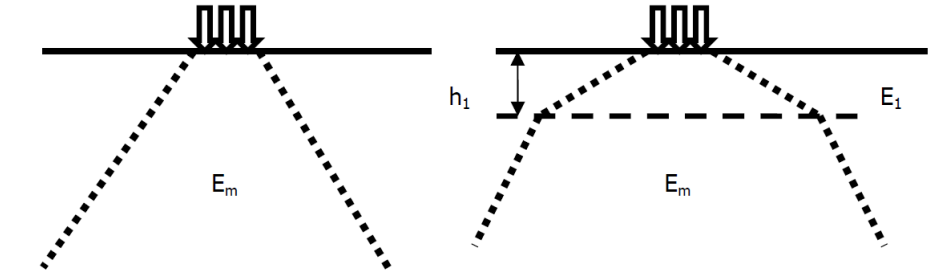

Figure 28: Effect of applying a stiffer top layer on the spreading of the load.

- In order to be able to calculate stresses in such two layered systems, Odemark's equivalency theory [13] is of help. The idea behind Odemark's theory is that the vertical stresses at the interface between the top layer with stiffness E_1 and thickness h_1 and the half space with stiffness E_m are the same as the stresses at an equivalent depth h_{eq} with stiffness E_m. This principle is shown in figure 29.

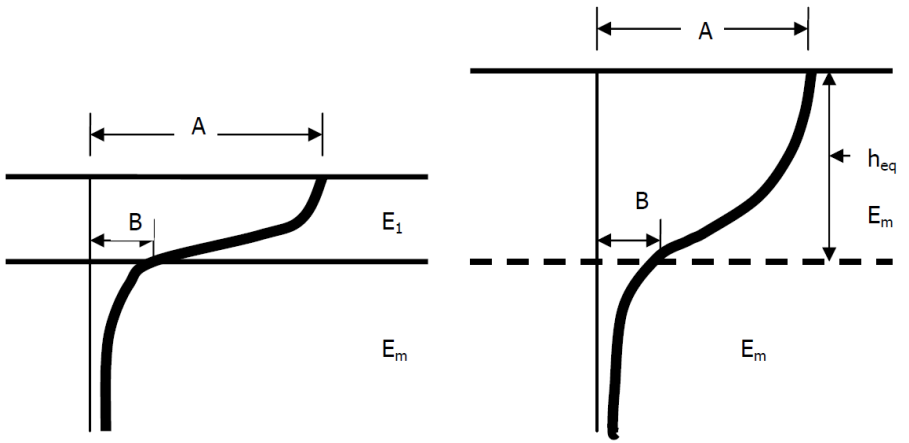

Figure 29: Principle of Odemark's equivalency theory.

- The figure shows on the left hand side the distribution of the vertical stresses in a two layer system. On the right hand side the equivalent h_{eq} is shown resulting in the same vertical stress (B) at the interface between the top layer and the underlying half space. Odemark showed that the equivalent layer thickness can be calculated using:

$$h_{eq} = n\, h_1 (E_1 / E_m)^{0.33}$$

- If Poisson's ratio of the top layer equals Poisson's ratio of the half space, then n = 0.9.

- The question of course is how well this Odemark/Boussinesq approach allows accurate predictions of the vertical stresses in pavements to be made. As is shown in figure 30 [14], this approach seems to be fairly effective in case one is dealing with pavements having unbound bases and subbases.

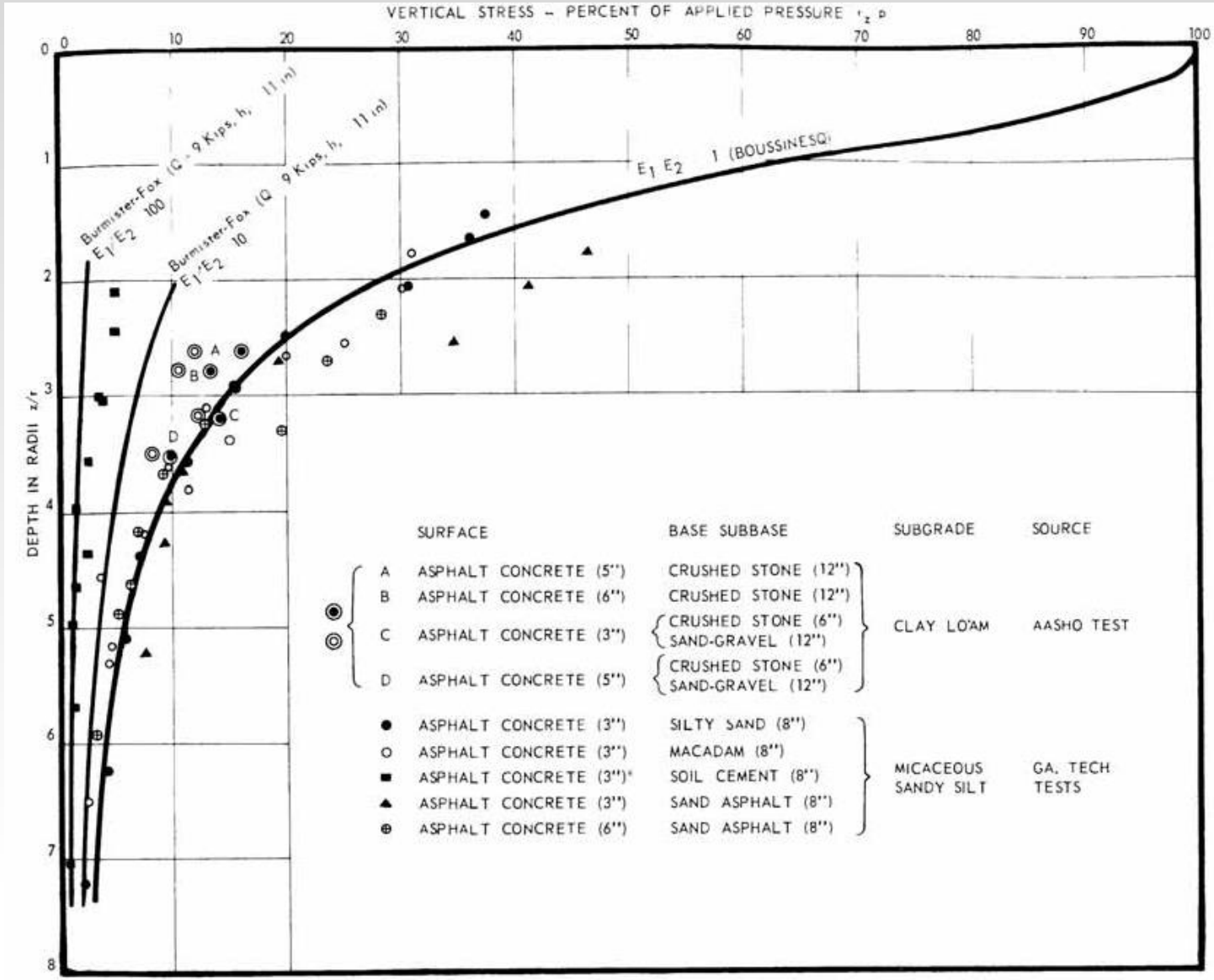

Figure 30: Comparison of measured and calculated vertical stresses in pavements.

- Let us illustrate the procedure by means of an example. We want to know the stresses in a homogeneous half space (modulus 100 MPa) that is loaded with a wheel load of 50 kN. Since the contact pressure is known to be 700 kPa, we can calculate the radius of the loading area following:

$$Q = \pi\, p\, a^2$$

Where:
p = contact pressure,
a = radius of the contact area,
Q = wheel load.

In this way we calculate a = 150 mm. If we assume Poisson's ratio to be 0.25, then we can derive from figure 27 that the vertical stress under the centre of the load at a depth of 150 mm (z = a) is to 60% of p being 420 kPa. Assume that this stress is too high and that a layer is placed on top of the half space having a modulus of 300 MPa and a thickness of 150 mm. The equivalent layer thickness of this layer is:

$$h_{eq} = 0.9\, h_1 (E_1 / E_m)^{0.33} = 0.9 * 150 * (300 / 100)^{0.33} = 194 \text{ mm}$$

We can now calculate the vertical stress using the same Boussinesq chart but this time the depth at which we have to determine the stress is 194 + 150 = 344 mm which is at a depth of z = 2.3 a. From figure 27 we notice that now the vertical stress is equal to approximately 20% of p being 140 kPa.

5.3 Stresses in two layer systems

- If the stresses in the subgrade, the half space, due to the wheel load are too high, a stiff top is needed to reduce these stresses. Such a system, a stiffer layer on top of a softer half space, is called a two layer system. It could represent e.g. a full depth asphalt pavement on top of a sand subgrade.

- Burmister [5] was the first one who provided solutions for stresses in a two layer system. Again, it is beyond the scope of these lecture notes to provide a detailed discussions on the mathematical background. Here only attention will be paid to the results of those mathematical analyses and how they can be used in practice.
- Figure 31 shows the effect of a stiff top layer on the distribution of the vertical stresses in a two layer system. First of all we notice that the distribution of the vertical stress is bell shaped. Furthermore we notice that the magnitude of the vertical stress is quite influenced by the stiffness of the top layer. The width of the stress bell however is much less influenced by the stiffness of the top layer.

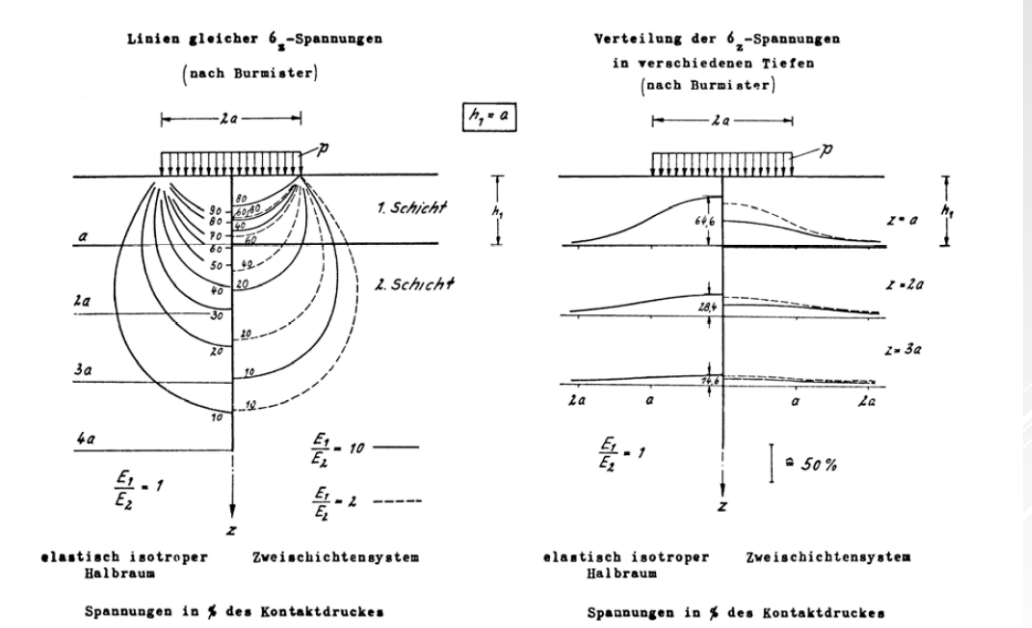

Figure 31: Distribution of the vertical stress in a one and two layer system.

- A stiff top layer not only provides protection to the second layer, also tensile stresses at the bottom of the top layer develop. These stresses are due to bending of the top layer. This implies that for two layer systems we are dealing with two design parameters being the horizontal tensile stress at the bottom of the top layer and the vertical compressive stress at the top of the second layer (figure 32).

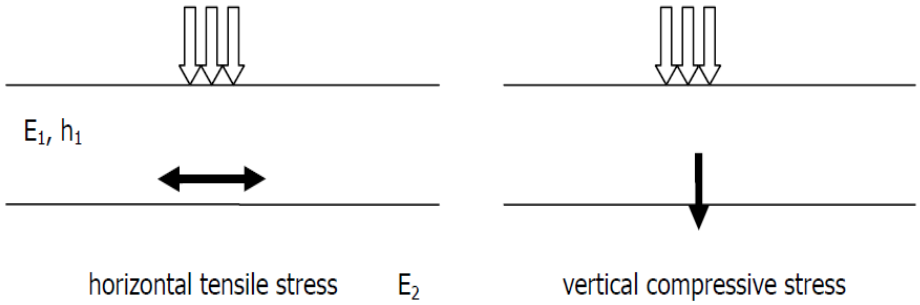

Figure 32: Design criteria in a two layer pavement system.

- If the horizontal tensile stress at the bottom of the top layer is too high, it will be the cause for cracking of the top layer. If the vertical compressive stress at the top of the bottom layer is too high, excessive deformation will develop in that layer.

- Figure 33 shows the distribution of the horizontal and vertical stresses in a two layer system under the centre of the load in relation to the ratio E_1 / E_2 and for h = a. Please note that Poisson's ratio is 0.25 for both layers.

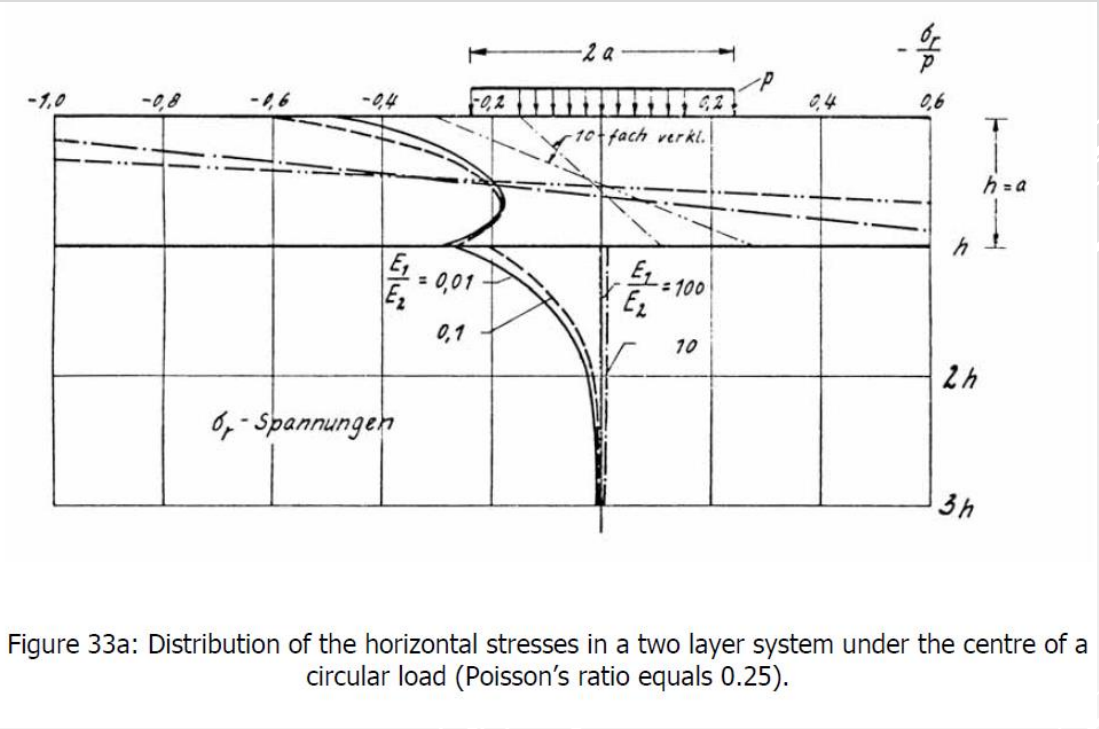

Figure 33a: Distribution of the horizontal stresses in a two layer system under the centre of a circular load (Poisson's ratio equals 0.25).

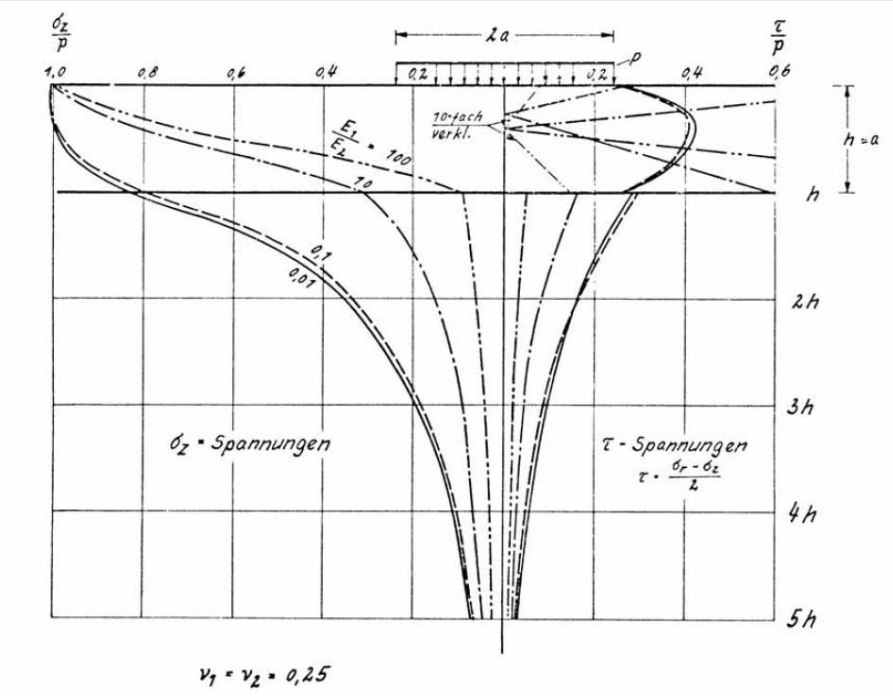

Figure 33b: Distribution of the vertical stresses in a two layer system under the centre of a circular load.

- From the figure 33a one can observe that significant horizontal stresses develop in the top layer. When $E_1 / E_2 = 10$, a tensile stress equal to the contact pressure p develops while this value becomes 2.7 * p when $E_1 / E_2 = 100$. One also observes that at those modulus ratio's the tensile stresses in the second layer can almost be neglected. Another interesting aspect is that the neutral axis is almost in the middle of the top layer for modulus ratio's of 10 and higher. Figure 33b shows that a stiff top layer greatly reduces the vertical stresses in the bottom layer. As we have seen in figure 27, the stress at a depth of z = a is 60% of the contact pressure in case of a half space. Figure 33b shows that if the modulus ratio is 10, the vertical stress at z = a is only 30% of the contact pressure.

- Let us go back for a moment to Odemark's equivalency theory. We have noticed that in a half space, the vertical stress at a depth of z = a under the centre of the load equals 60% of the contact pressure. If we assume that the top part of that half space is replaced over a depth of a by a material that has a 10 times higher modulus, than the equivalent layer thickness of that layer equals:

  $h_{eq} = 0.9 * a * (10)^{0.33} = 1.92 * a$

- From figure 27 we can determine that the vertical stress at that depth equals approximately 30% of p. This is in excellent agreement with the result obtained from figure 33b. This is considered to be proof of the validity of Odemark's approach.

- Until now no attention has been paid to the conditions at the interface. From our structural design classes we know that it makes quite a difference whether layers are perfectly glued to each other and there is no slip (full friction) between the layers or whether the layers can freely move over each without any friction (full slip). The effect of those two interface conditions on the stresses at the bottom of the top layer are shown in figure 34.

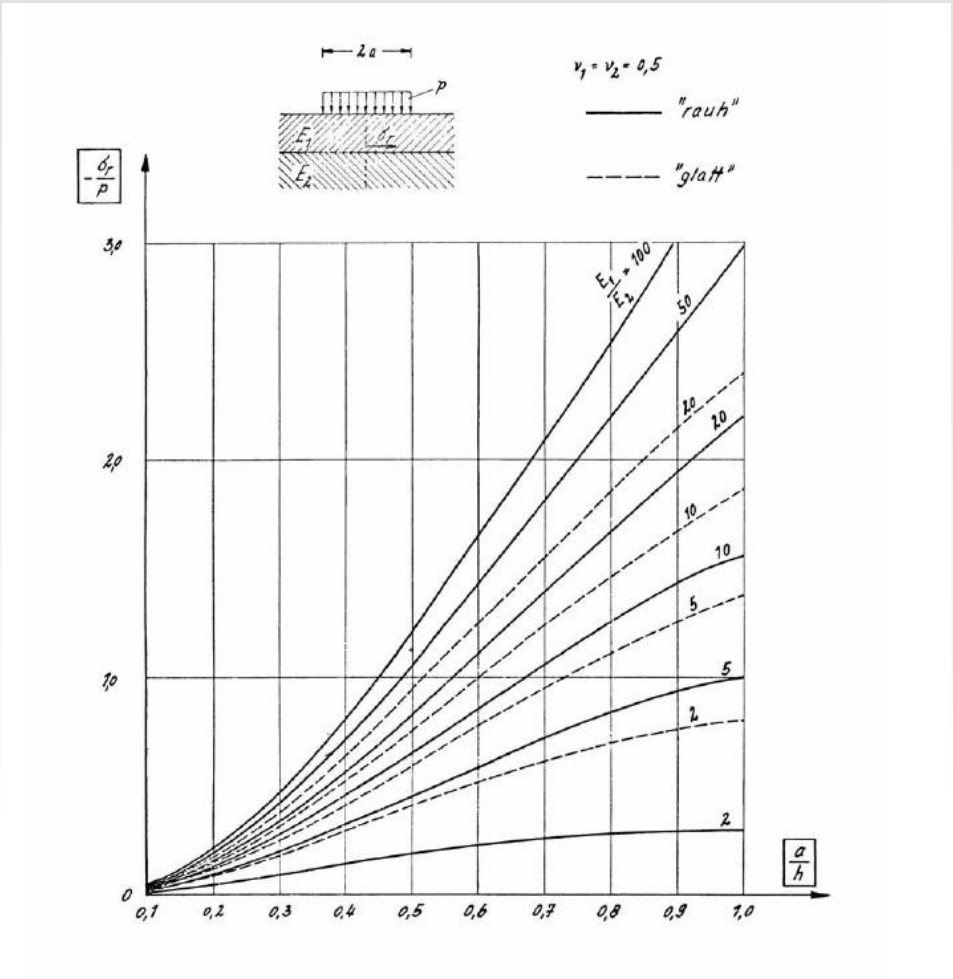

Figure 34a: Influence of friction on the radial stresses at the bottom of the top layer under the wheel centre (please note that Poisson's ratio is 0.5).

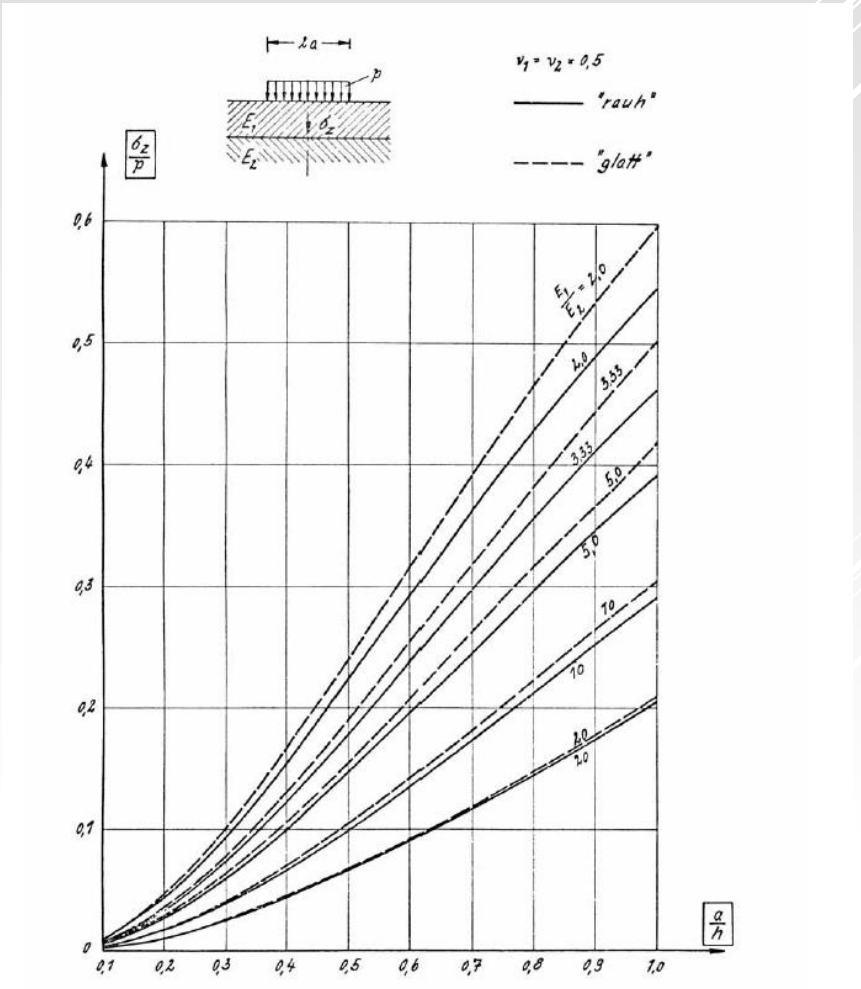

Figure 34b: Influence of friction on the vertical stress at the top of bottom layer under the wheel centre (please note that Poisson's ratio is 0.5).

- As one will observe, the presence of friction has a significant influence on the radial (horizontal) stress at the bottom of the top layer especially at low values for the ratio E_1/E_2. We also note that the influence on the vertical stress is much smaller.

- If there is full friction or full bond at the interface, the following conditions are satisfied.

a. The vertical stress just below and above the interface are equal because of equilibrium, so:

$\sigma_{z\ \text{bottom, top layer}} = \sigma_{\text{top, bottom layer}}$

b. The horizontal displacements just above and below the interface are the same because of full friction, so:

$u_{r\ \text{bottom, top layer}} = u_{r\ \text{top, bottom layer}}$

c. The vertical displacements just above and below the interface are the same because of continuity, so:

$u_{z\ \text{bottom, top layer}} = u_{z\ \text{top, bottom layer}}$

In case of full slip, only conditions a. and c. are satisfied.

- Another important factor is Poisson's ratio. Since measurements needed to determine Poisson's ratio are somewhat complicated, values for this parameter are usually estimated from information available from literature. The question then is to what extent wrong estimates influence the magnitude of the stresses. Information on this can be found in figure 35. Figure 35a e.g. shows that the influence of Poisson's ratio on the radial stress at the bottom of the asphalt layer is quite significant. This also means that it will have a significant influence on the radial strain. As one can see from figure 35b, the influence of Poisson's ratio on the vertical stress at the top of the bottom layer is limited.

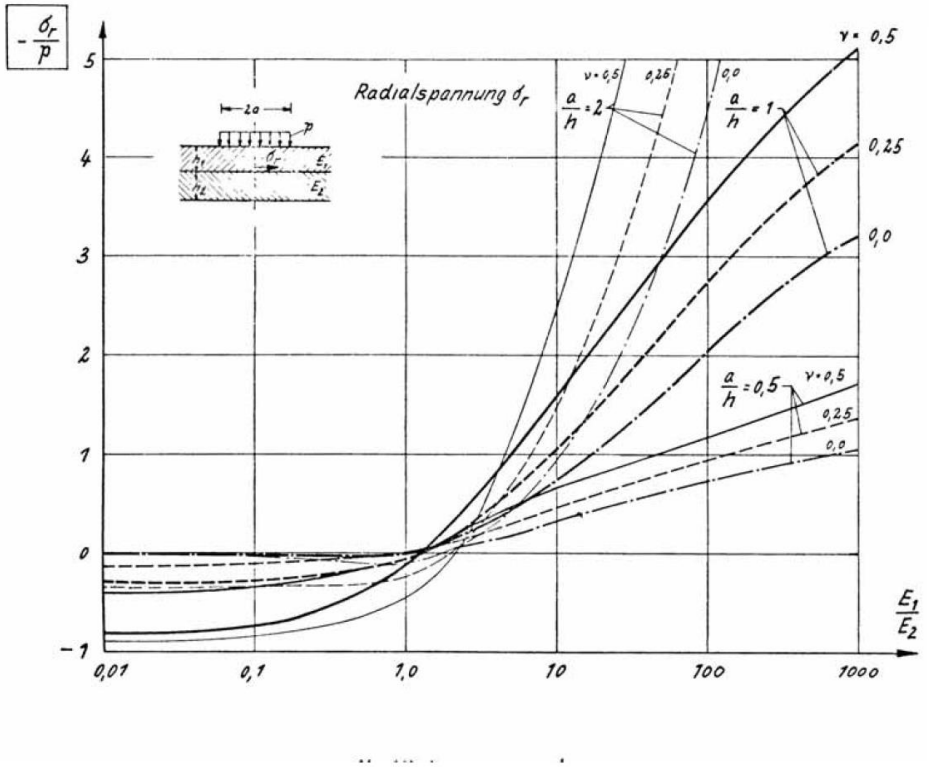

Figure 35a: Influence of Poisson's ratio on the radial stress at the bottom of the top layer.

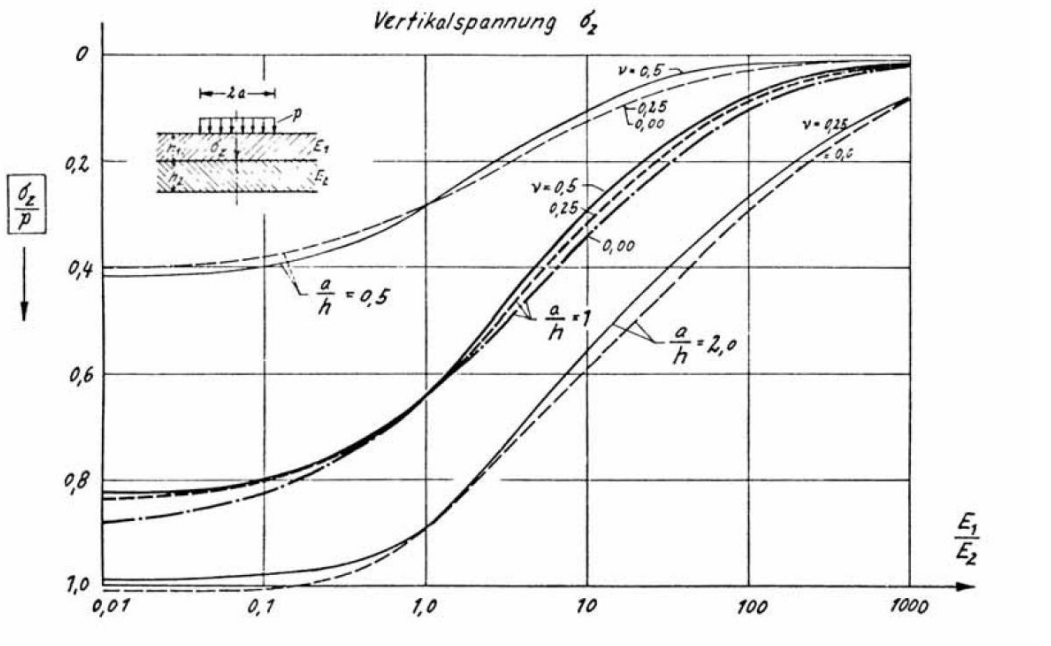

Figure 35b: Influence of Poisson's ratio on the vertical stress at the top of the bottom layer.

- By means of the figures available we now can estimate the stresses and strains in two layer pavements. This will be illustrated by means of the following example.

Assume we have a two layer structure consisting of a 150 mm thick asphalt layer on top of a sand subgrade. The elastic modulus of the asphalt layer is 5000 MPa while the modulus of the sand layer is 100 MPa. A 50 kN wheel load is applied on the pavement. The contact pressure 700 kPa which results in a radius of the circular contact area of 150 mm. Poisson's ratio for both the asphalt and the sand layer equals 0.35. We want to know the stresses and strains in the locations indicated below.

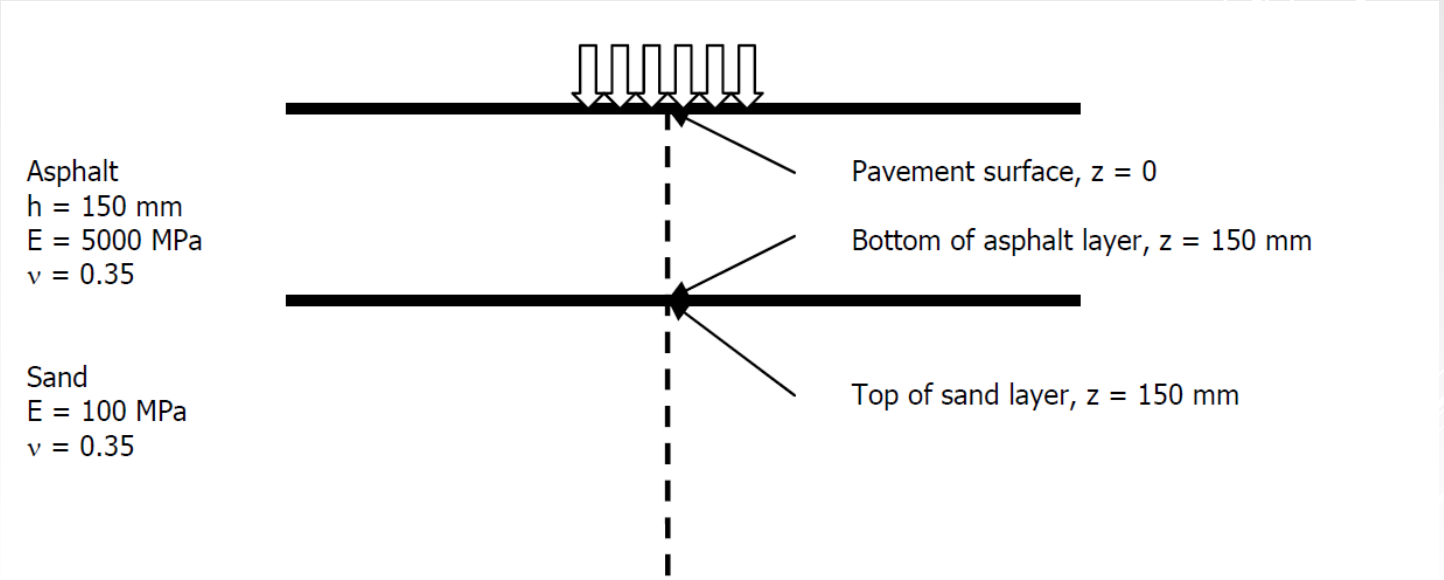

Figure 36: Two layer pavement example problem.

- Let us start with the calculation of the stresses and strains at the bottom of the asphalt layer. Since both layers have a Poisson ratio of 0.35, we have to use figure 35 and interpolate between the lines for v = 0.25 and v = 0.5. Since E1 / E2 = 50 and a / h = 1 we read from the graphs shown in figure 37 that -σr / p = 2.7 and σz / p = 0.15. Since the contact pressure is a compressive stress and we decided to express compression by means of the minus sign (-), we calculate σr = σt = 1890 kPa and σz = -105 kPa.
- Please note that under the centre of the load centre there is not only a horizontal radial stress σr but also a horizontal tangential stress σt (see also figure 26). These stresses are acting perpendicular to each other and because the load centre is in the axis of symmetry, the tangential stress is equal to the radial stress.

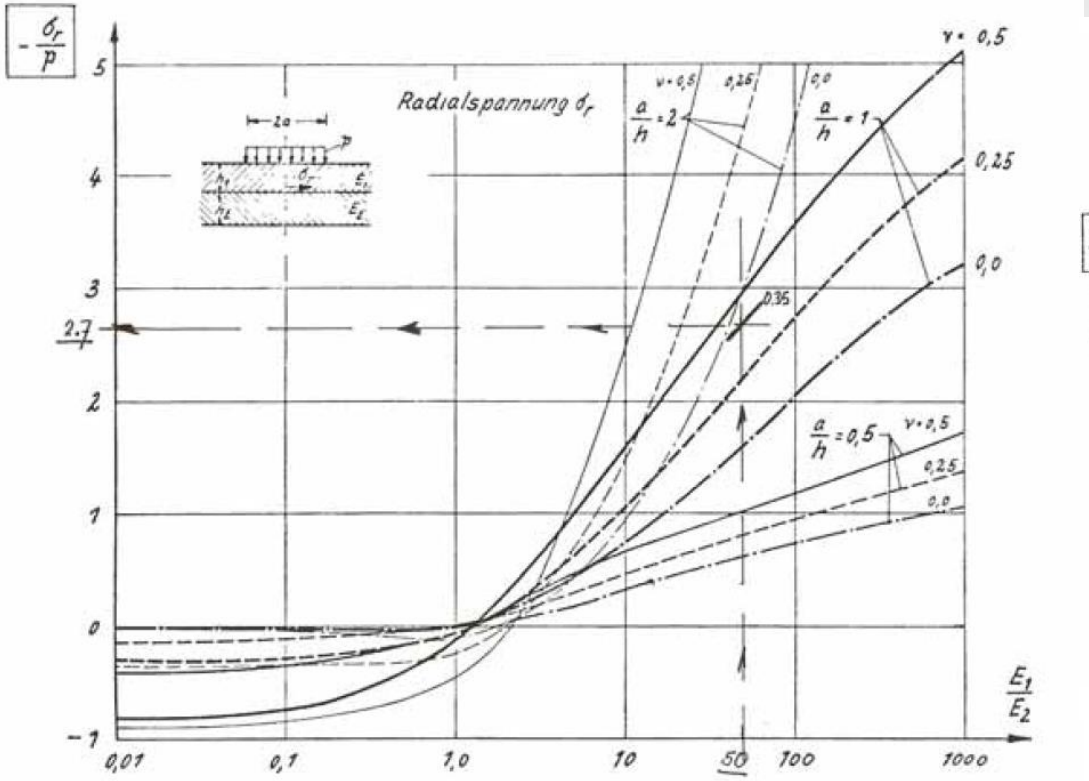

Figure 37a: Estimation of the horizontal stress at the bottom of the asphalt layer.

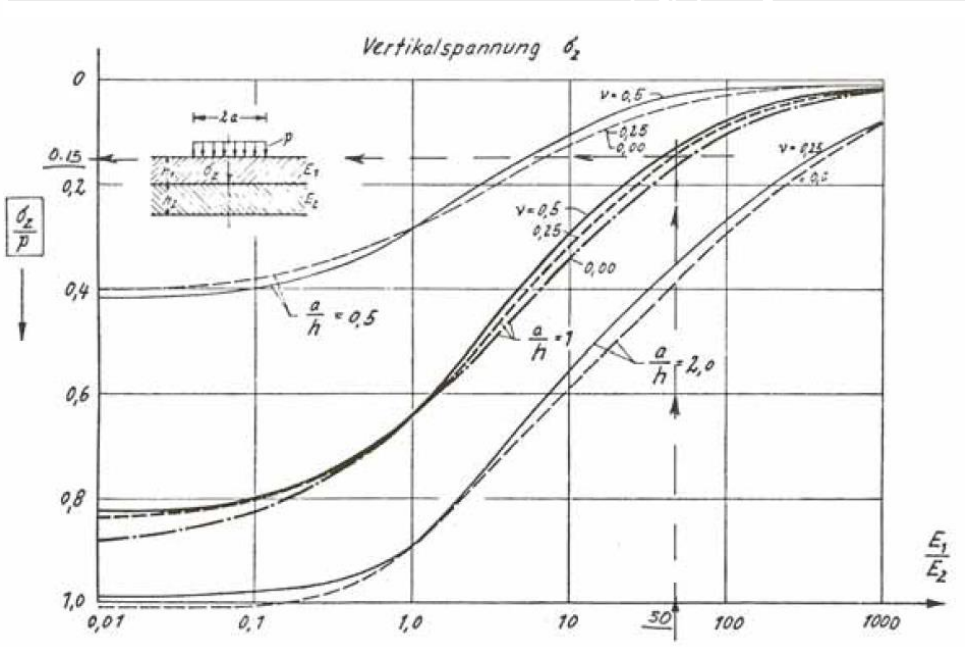

Figure 37b: Estimation of the vertical stress at the top of the subgrade.

The strains are calculated as follows:

$\varepsilon r = \varepsilon t = (\sigma r - \nu\sigma t - \nu\sigma z) / E = (1890 – 0.35 * 1890 – 0.35 * -105) / 5000000 = 2.53 * 10^{-4}$

$\varepsilon z = (\sigma z - \nu\sigma r - \nu\sigma t) / E = (-105 – 0.35 * 1890 – 0.35 * 1890) / 5000000 = -2.86 * 10^{-4}$

Please note that the units used for the stresses and elastic modulus is kPa. This implies that the value of 5000000 is used for the modulus (originally it was given in MPa).

- Let us now consider the stresses and strains at the top of the asphalt layer. We notice that figure 35 is not of help anymore because that figure only gives information about the stresses at the bottom of the asphalt layer. We know however that, for reasons of equilibrium, the vertical stress at the top of the asphalt layer is equal to the contact pressure, so $\sigma z = -700$ kPa. There are no graphs available to estimate the horizontal stress at the top of the asphalt layer for $\nu = 0.35$, but we can make a reasonable estimate of those stresses. From figure 35 we determine that the tensile stress at the bottom of the asphalt layer is $-2.2 * p$ if $\nu = 0.25$. If we insert that value in figure 33, then we can determine that the radial stress at the top of the pavement equals $2.5 * p$ (see figure 38).

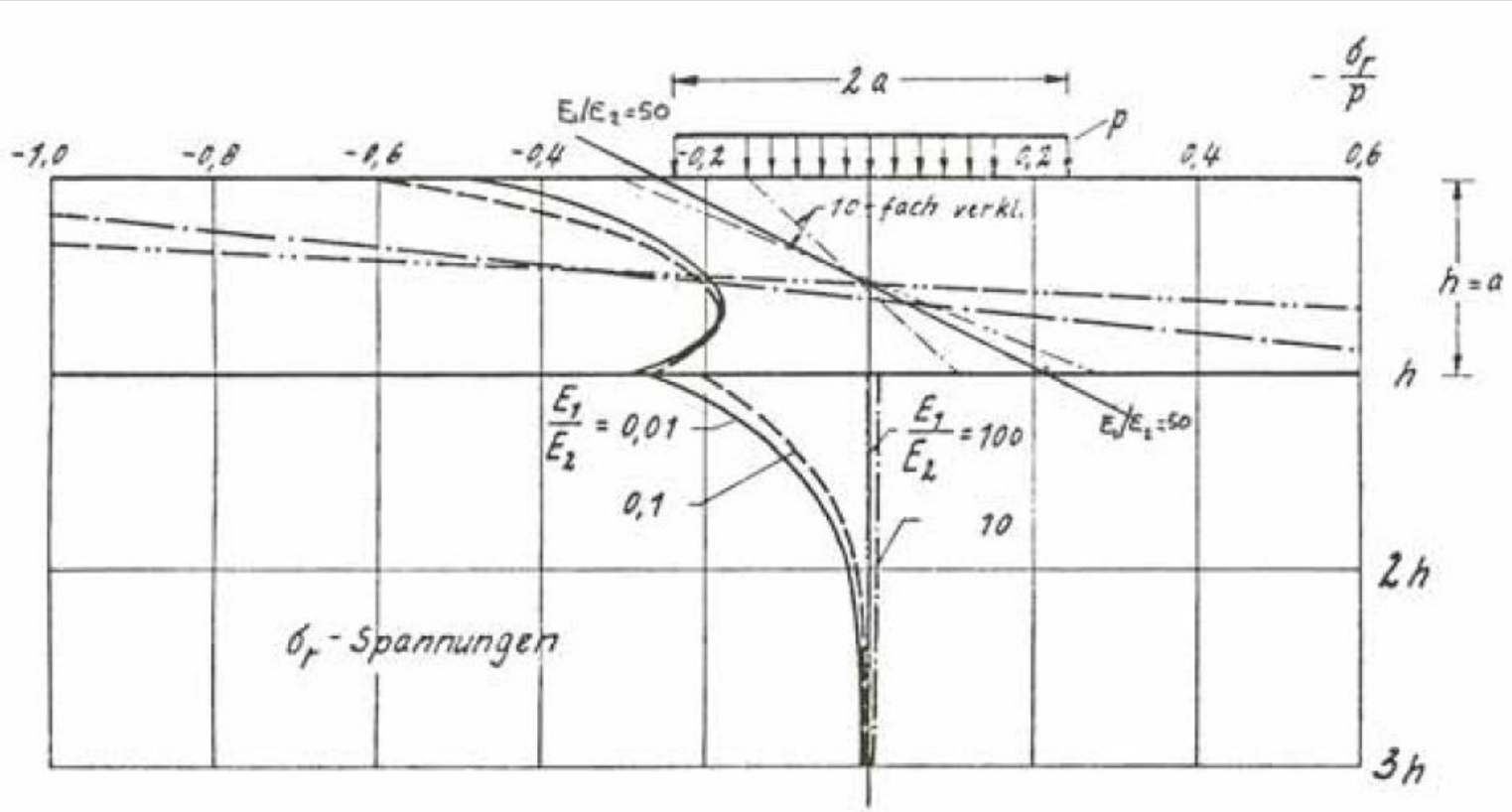

Figure 38: Estimation of the horizontal stress at the top of the asphalt layer.

- Going back to figure 35a we notice that the radial stresses at the bottom of the asphalt layer are 2.7 * p / 2.2 * p = 1.23 times higher when v = 0.35 instead of 0.25. Therefore we estimated the radial compressive stress at the top of the asphalt layer to be 1.27 * 2.5 * p = -2223 kPa (the – sign is because p is compressive). Using these values we calculate:

$\varepsilon r = \varepsilon t = (\sigma r - \nu\sigma t - \nu\sigma z) / E = (-2223 - 0.35 * -2223 - 0.35 * -700) / 5000000 = -2.4 * 10^{-4}$

$\varepsilon z = (\sigma z - \nu\sigma r - \nu\sigma t) / E = (-700 - 0.35 * -2223 - 0.35 * -2223) / 5000000 = 1.71 * 10^{-4}$

This later value implies that a vertical tensile strain develops at the top of the asphalt layer!

- Finally we will discuss the stresses and strains at the top of the subgrade.

Because of equilibrium, the vertical stress at the top of the subgrade is equal to the vertical stress at the bottom of the asphalt layer being -105 kPa. Also in this case we have no graphs available to estimate the horizontal stresses at the top of the subgrade. Nevertheless figure 33a is showing that the radial stress at the top of the subgrade is very small and almost zero for E1 / E2 = 100. For that reason we assume that at the top of the subgrade $\sigma r = \sigma t = 0$.

Using these values we calculate:

$\varepsilon r = \varepsilon t = (\sigma r - \nu\sigma t - \nu\sigma z) / E = (0 - 0 - 0.35 * -105) / 100000 = 3.68 * 10^{-4}$

$\varepsilon z = (\sigma z - \nu\sigma r - \nu\sigma t) / E = (-105 - 0 - 0) / 100000 = -1.05 * 10^{-3}$

5.4 Stresses in three layer systems

- The calculation of the stresses and strains in three layer systems is based on the same principles as used for two layer systems. It is however much complicated to derive tables [7] and charts [8] that allow the stresses at various points in the pavement to be estimated and as we will see from the given examples, those charts are not very user friendly.

- Figure 39 shows the stresses and locations in a three layer system for which tables and graphs have been developed. Note that a Poisson's ratio of 0.5 was used for all layers.

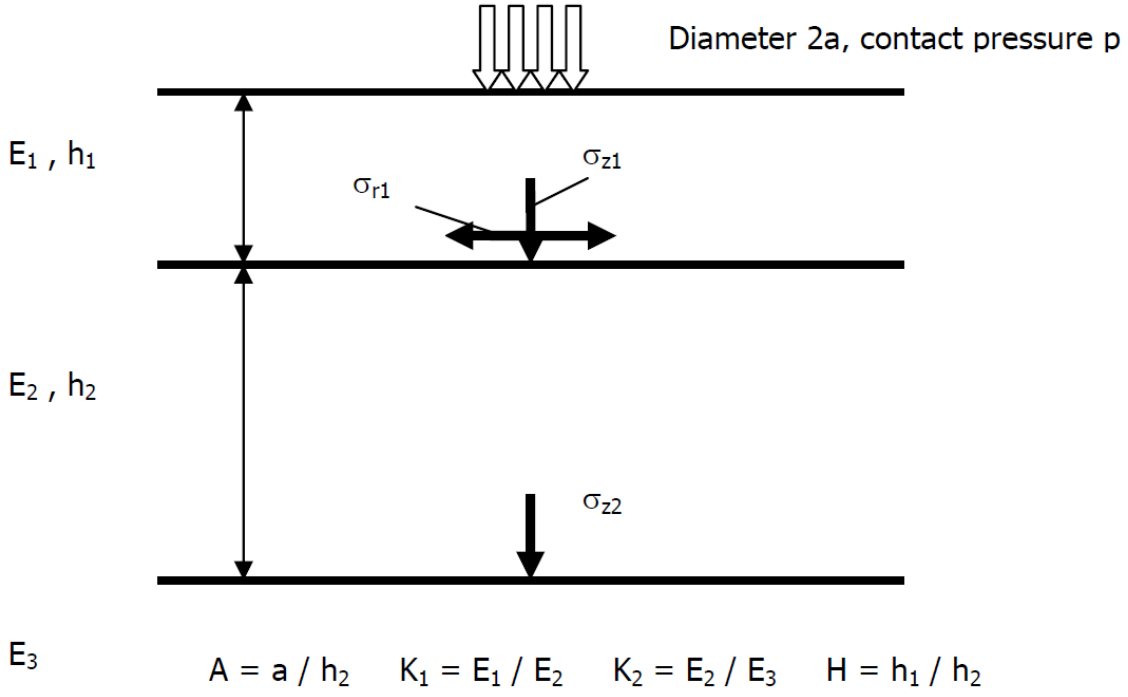

Figure 39: Locations in a three layer system for which tables and graphs to estimate stresses have been developed.

- In developing those tables and graphs, the following parameters have been used.

$A = a / h_2$; $H = h_1 / h_2$; $K_1 = E_1 / E_2$; $K_2 = E_2 / E_3$

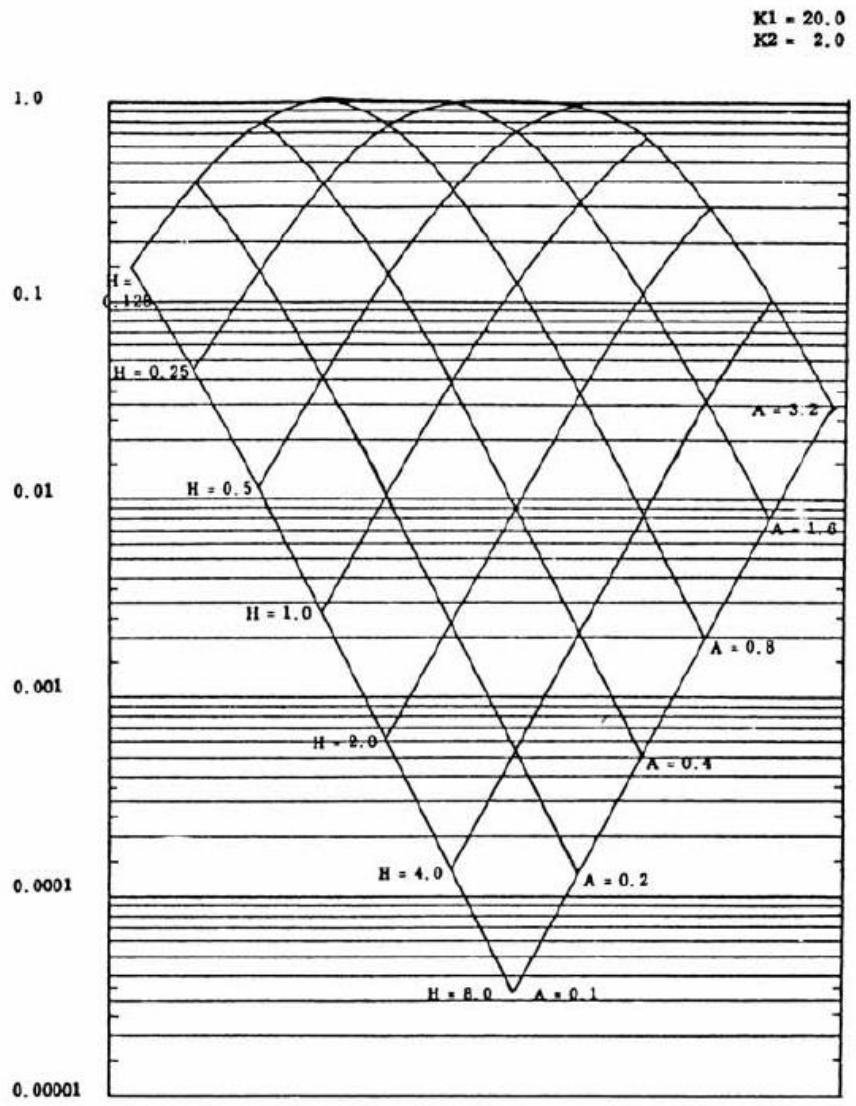

Figure 40: Chart to estimate σ_{zz1} (vertical stress at the top layer – base interface) in a three layer system.

- Figures 40, 41 and 42 show the graphs for the estimation of resp. σ_{zz1}, σ_{zz2}, and σ_{rr1} for $K_1 = 20$ and $K_2 = 2$.

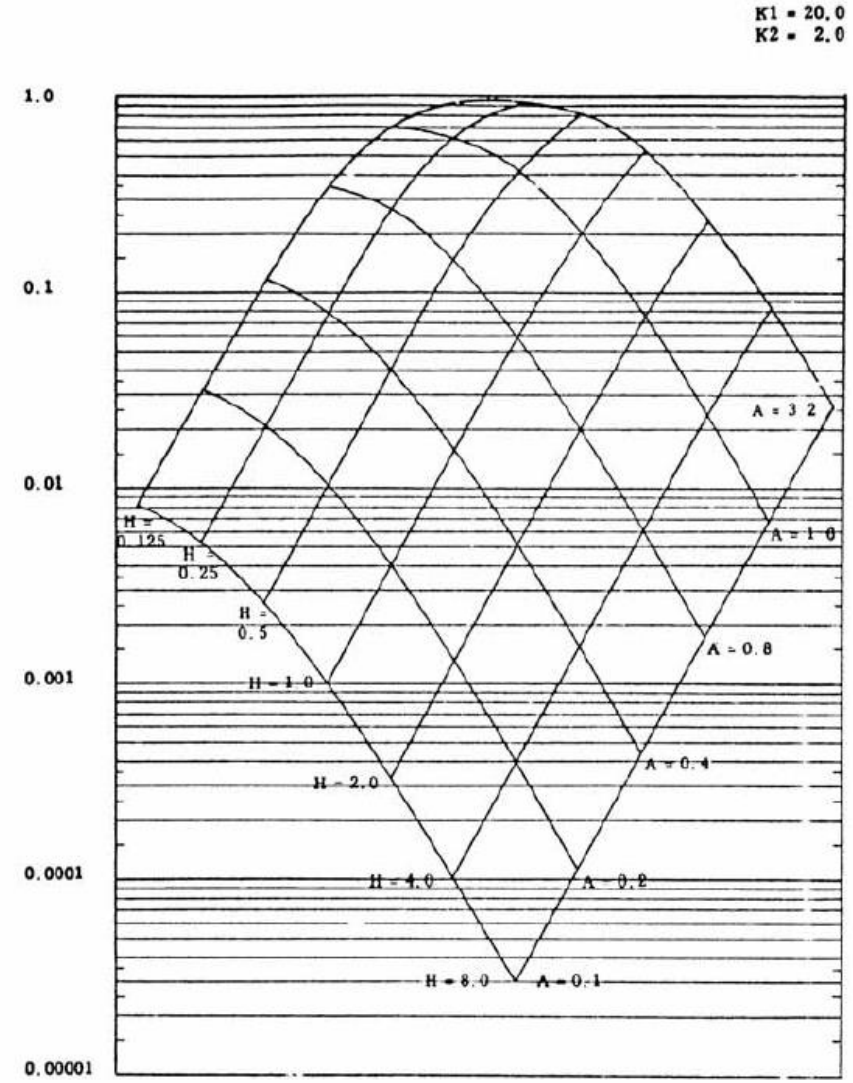

Figure 41: Chart to estimate σ_{zz2} (vertical stress at the base – subgrade interface) in a three layer system.

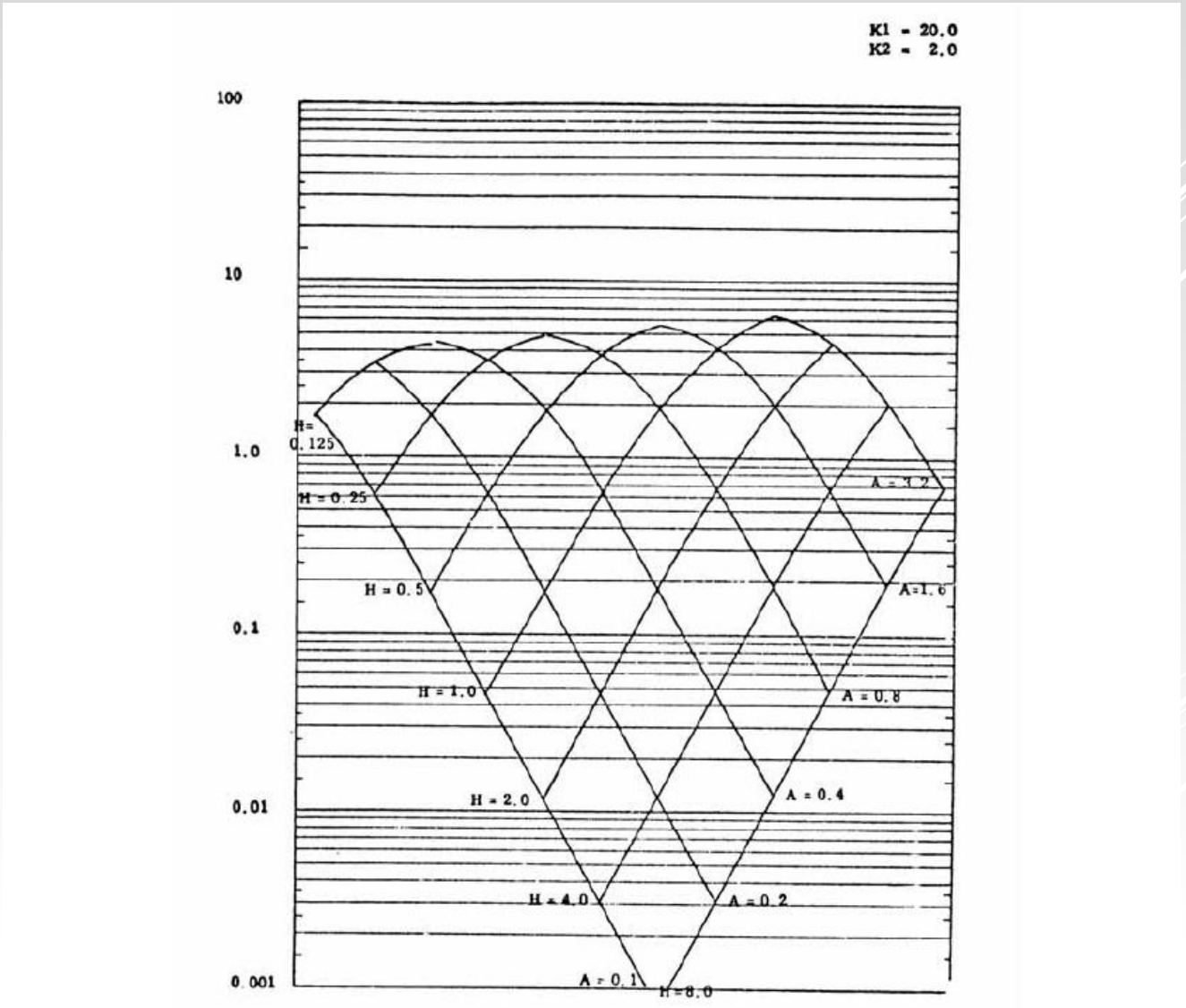

Figure 42: Chart to estimate σ_{rr1} (horizontal stress at the bottom of the top layer at the top layer – base interface) in a three layer system.

The use of the charts is illustrated by means of an example. Let us assume we have a three layer system consisting of 100 mm of asphalt (E = 6000 MPa) that is placed on a 300 mm thick base (E = 300 MPa) on a subgrade with a stiffness with E = 150 MPa. The magnitude of the load is 50 kN and the radius of the loaded area is 150 mm. This implies that the contact pressure is 700 kPa.
This input means that K1 = 20, K2 = 2, A = 2 and H = 0.33. We want to know the horizontal stress at the bottom of the asphalt layer. Using figure 42 in the way as illustrated in figure 43, we derive that the horizontal stress factor is approximately 7 which results in σrr1 = 7 * 700 = 4900 kPa.

- It is obvious that the determination of the stresses in this way is a quite time consuming approach especially since most of the time interpolations have to be made between the different charts. Furthermore the charts are only valid for Poisson's ratio equals 0.5 and most materials have a different value for this parameter. Therefore use of one of the many computer programs that are available nowadays is highly recommended.

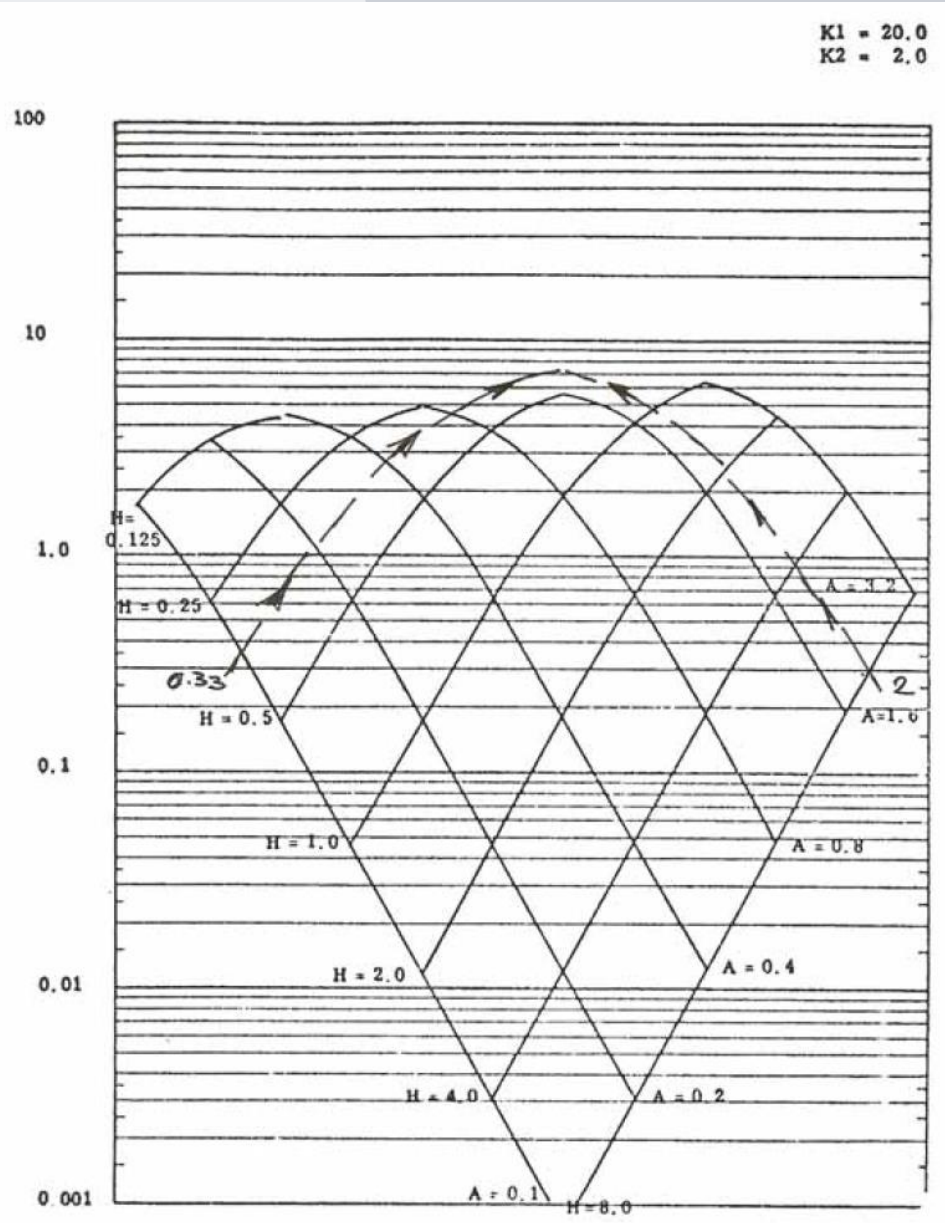

Figure 43: Example of the estimation of σ_{rr1}.

5.5 Stresses due to horizontal loads

- It is obvious that in reality not only vertical stresses are applied on the pavement surface. Also horizontal shear stresses are present, acting in the longitudinal and transverse direction. These shear stresses are due to traction forces, braking, cornering etc. They occur under free rolling as well as driven tires. As we will see in the next chapter, the real stress conditions in the contact area are indeed very complex.
- Several researchers have studied the effect of such shear forces and early work on this topic is done by Verstraeten [15] and Wardle and Gerrard [16]. Given the limited computational power in those days, they had to apply rigorous simplifications of the real stress conditions. Nevertheless, a good idea of the effect of these shear stresses can be obtained from their work.
- Figures 44, 45 and 46 are taken from the work presented by Verstraeten. The figures show that depending on the applied shear force, significant radial and tangential stresses can develop at the pavement surface.
- Furthermore the figures show that the ratio of stiffness of the top layer over the stiffness of the second layer has a large effect on the magnitude of these stresses. It will be obvious that the ratios h1/a and h2/h1 will have a significant effect on the stresses at the interface

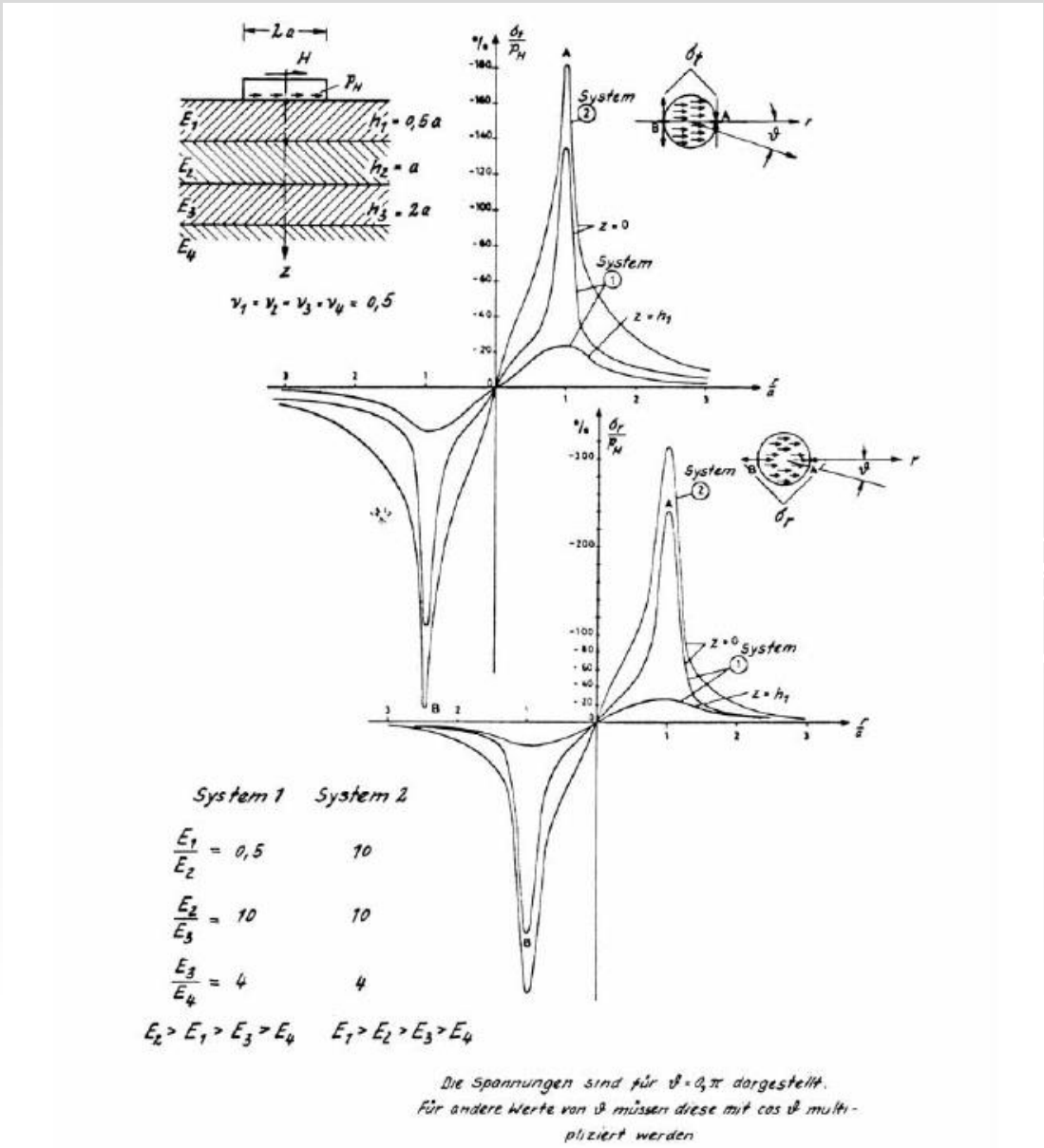

Figure 44: Radial and tangential stresses in a pavement system due to a uniformly distributed, unidirectional, shear load.

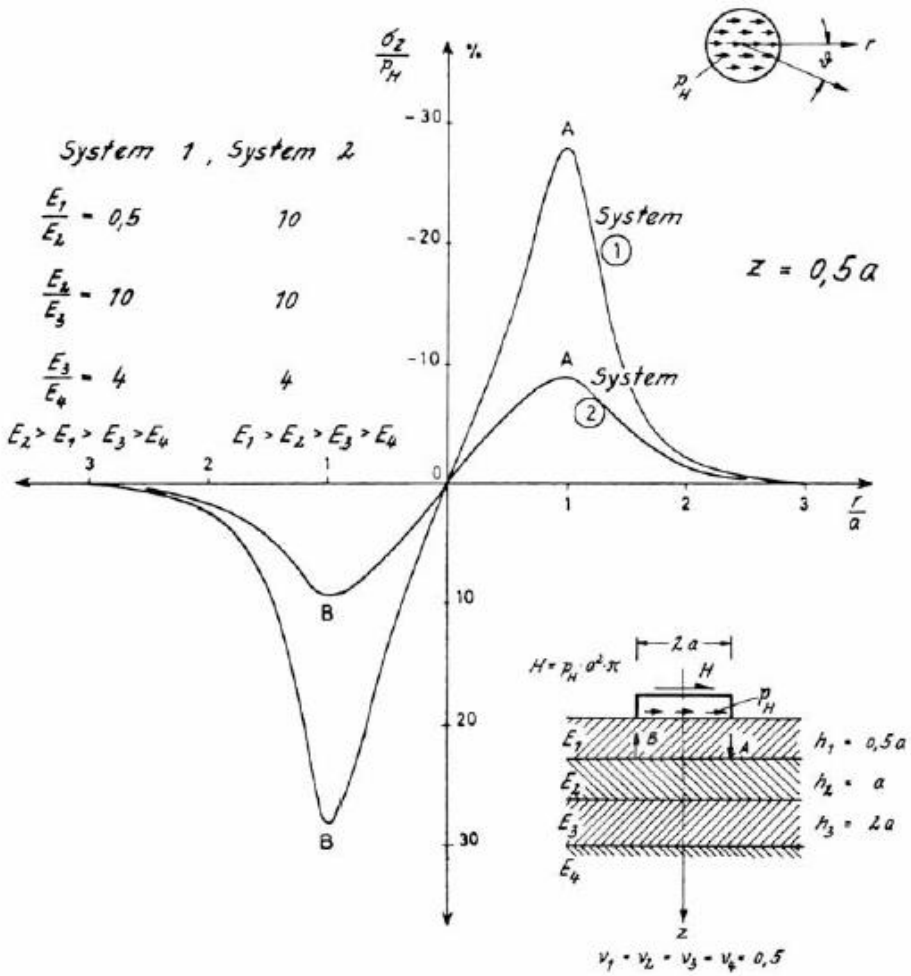

Figure 45: Vertical stresses in a pavement system due to a uniformly distributed, unidirectional shear load.

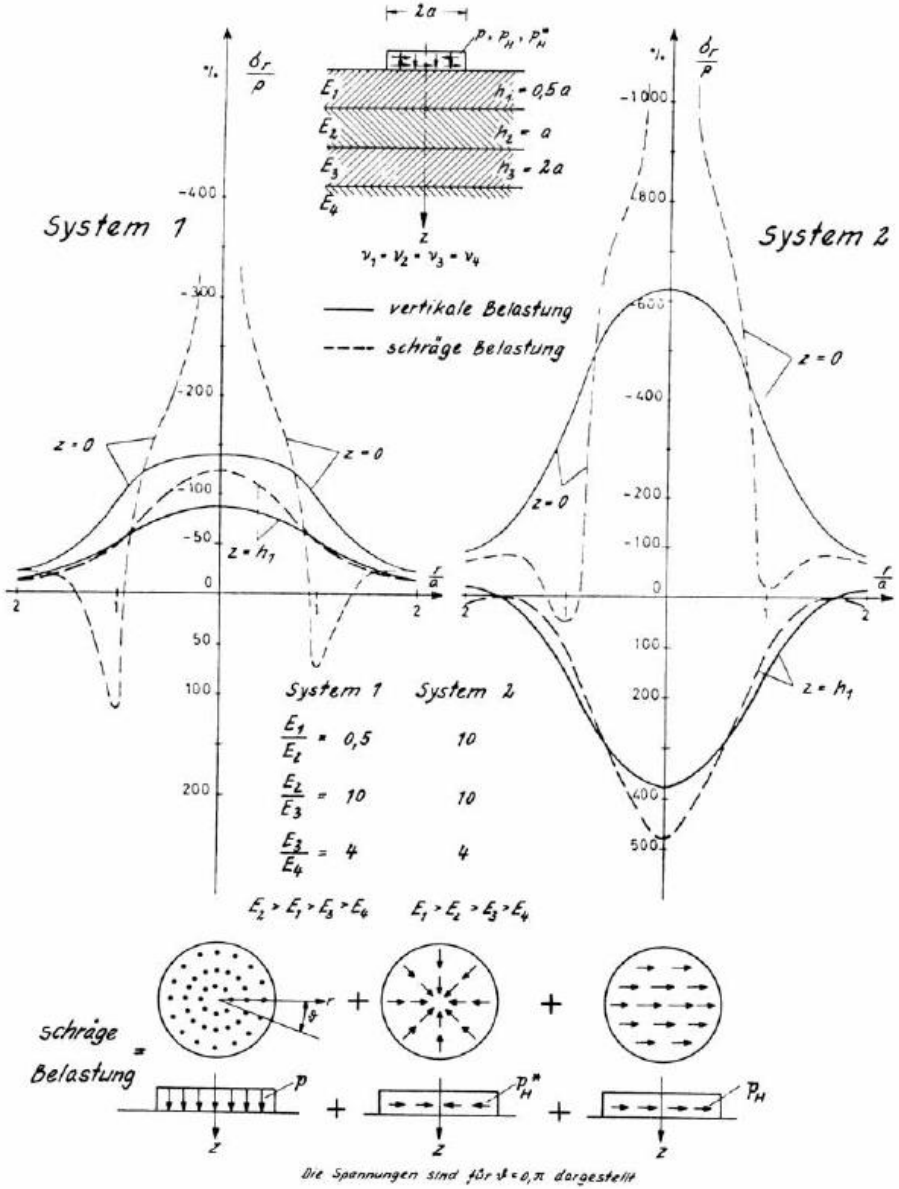

Figure 46: Radial stresses in a pavement system due to a combination of vertical stresses and uniformly distributed, unidirectional and multidirectional, shear forces.

5.6 Stresses in multilayer systems, available computer programs

As has been mentioned in the previous section, it is strongly recommended to use a multilayer computer program for the analysis of stresses and strains in three layer systems. This becomes a necessity in case the number of layers is 4 or more. Charts for the assessment of stresses in a four layer systems even don't exist. Many computer programs have been developed in time and it is almost impossible to give a complete picture of the available programs. Well known programs are BISAR, KENLAYER, CIRCLY, and WESLEA.

- BISAR and WESLEA only allow linear elastic materials to be taken into account.
- CIRCLY on the other hand allows taking into account anisotropic behavior of materials.
- Many of these programs have been incorporated in design systems such as the Shell Pavement Design System, CARE (developed in the Netherlands), mePADS (developed in South Africa).

- KENLAYER is an interesting system because it allows taking into account the stress dependent behaviour of unbound granular materials and soils.
- RUBICON, a program developed in South Africa, is a finite element based program that also allows to take into account the stress dependent behavior of granular materials. Furthermore this program allows probabilistic analyses to be made.
- Many of these programs can be found on the internet and can be retrieved for free while other software packages (mainly the design systems) have to be purchased.

It is beyond the scope of these lecture notes to discuss all the available programs in detail. In this part of the lecture notes we only discuss the output that is generated by computer programs that just calculate the stresses and strains in the pavement system due to traffic loads. In order to do so we will use the output as provided by BISAR developed by Shell. First of all however attention is paid to the "quality" of such programs.
It is generally accepted that the BISAR program can be taken as the reference to which all other programs can be compared. This is because of the high mathematical stability of the BISAR program. Quite some programs have minor flaws of which the user should be aware before using them. To check whether these flaws exist the stresses, strains and displacements have to be calculated in a number of points of the pavement structure (see figure 47).

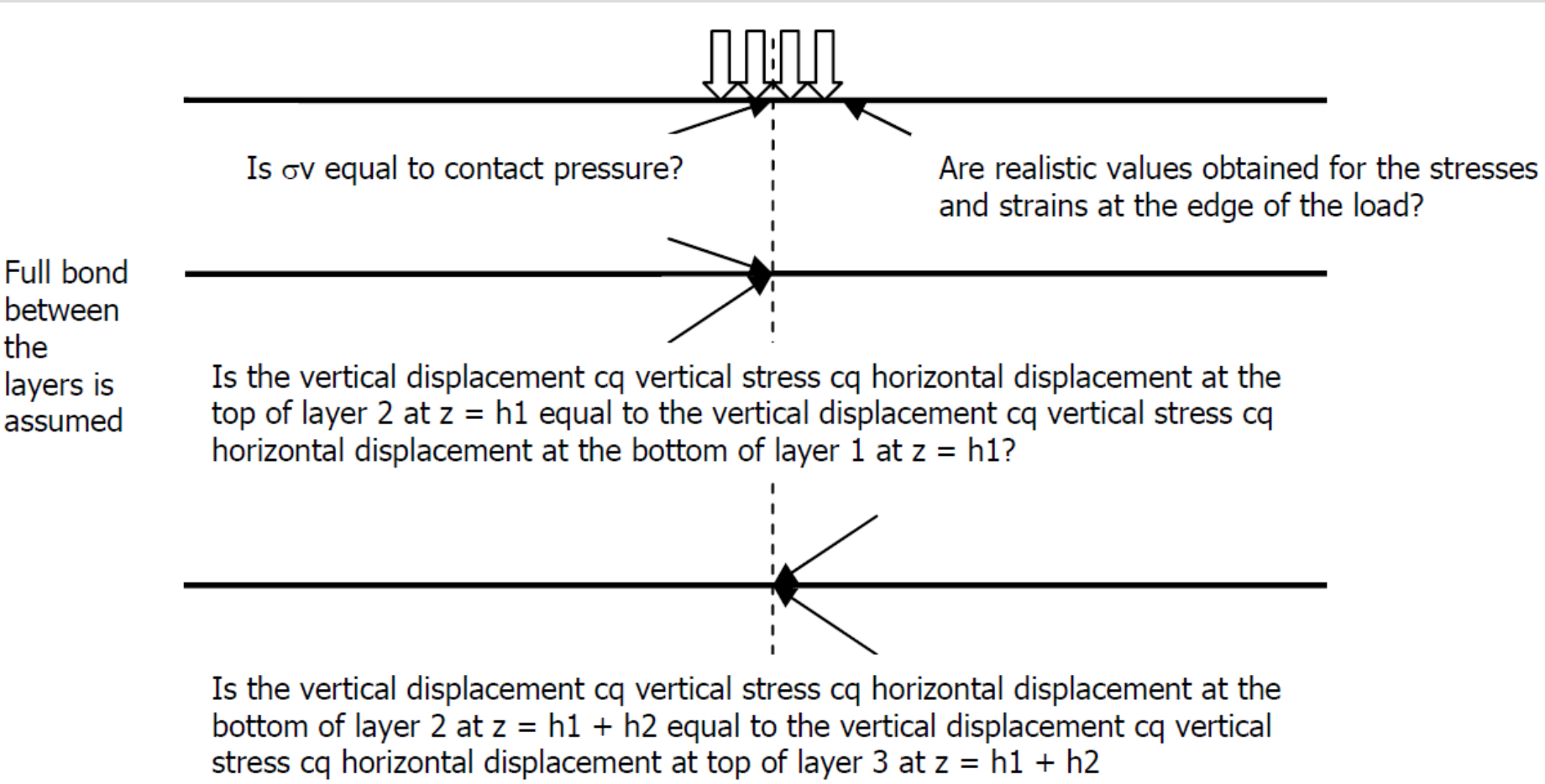

Figure 47: Locations in the pavement where consistency checks can be made.

- Some programs do not fulfill the requirements set for the interface between layers 1 and 2 or the interfaces between layers 2 and 3. These programs often also not fulfill the equilibrium requirement at the pavement surface under the centre of the load. More programs generate unrealistic results at the edge of the load. The problems at the interfaces and under the centre of the load at the pavement surface can easily be overcome by not requiring output at those interfaces but at locations that are e.g. 1 mm above or below the interface. Almost all programs generate comparable results if stresses and strains are required at other locations in the pavement.

Although most of the problems mentioned above can be overcome quite easily, one must be aware of the fact that some programs have difficulties in generating realistic results for pavements with a thin asphalt layer that has a low modulus on top on a thick stiff (high modulus) base layer (so if $h_1 / h_2 < 1$ and $E_1 / E_2 < 1$). It should be noted that the BISAR program passes all these requirements. Let us now return to the output that is generated by these computer programs and let us explain the output that is generated by BISAR for two example problems. The two problems that are analyzed are schematically shown in figure 48.

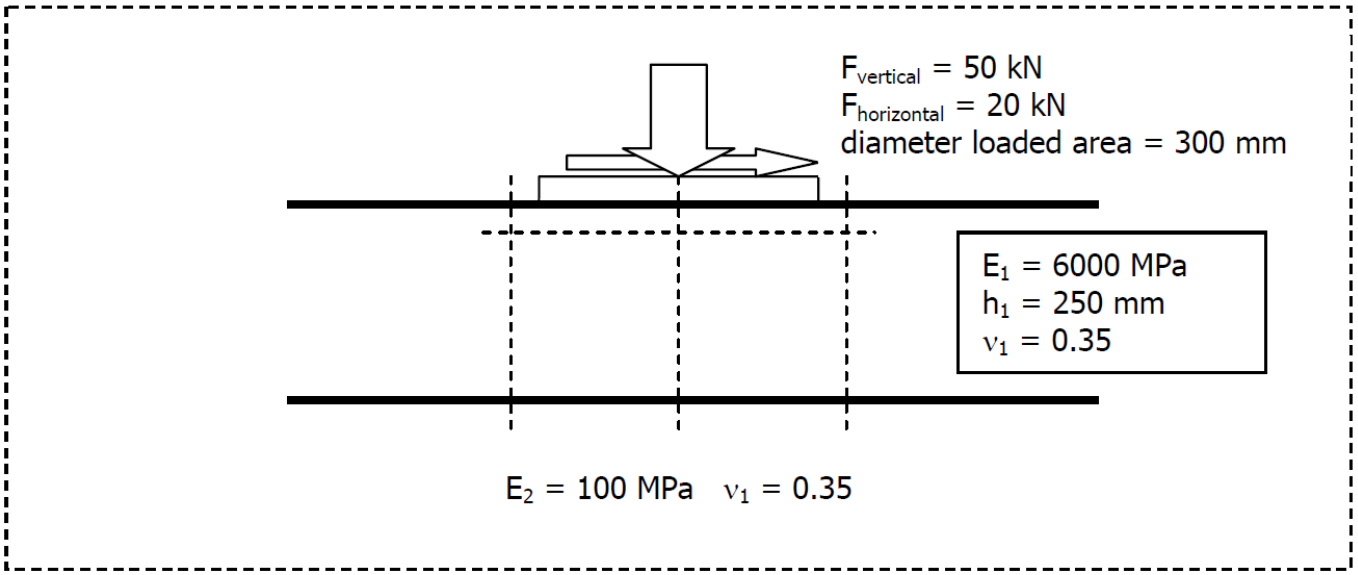

Figure 48a: Example problem.

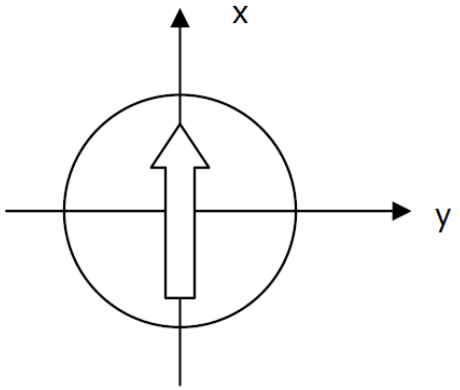

Figure 48b: Coordinate system and direction of the shear force as used in the example problem.

In the first example, only the vertical load is applied while in the second example the vertical and horizontal load is applied. The horizontal load acts in the x-direction and simulates a braking force. The stresses and strains are requested at the following x, y and z coordinates.

Load	Sheet	Layer	X [mm]	y [mm]	z [mm]
Vertical force only	2	1	0	0	0
	3	1	152	0	0
	4	1	152	0	10
	5	1	0	0	250
	6	2	0	0	250
Vertical and horizontal force	8	1	-152	0	0
	9	1	0	0	0
	10	1	152	0	0
	11	1	-152	0	10
	12	1	0	0	10
	13	1	152	0	10
	14	1	0	0	250
	15	2	0	0	250

Table 5: Locations where results are obtained.

Note: The sheet number refers to the handwritten numbers written on the output pages given in figure 49.

Please note that at the pavement surface and at a depth of 10 mm, the results are requested just outside the loaded area and at the load centre. This is done to determine the effect of the shear forces. In figure 49 all the calculation results are given while the main results are summarized in table 6.

Sheet nr.	σ_1 [Pa]	σ_2 [Pa]	σ_3 [Pa]	ε_1	ε_2	ε_3
2	-7.074E+05	-1.251E+06	-1.251E-6	2.800E-05	-9.421E-05	-9.241E-05
3	0	-4.231E+05	-6.758E+05	6.410E-05	-3.110E-05	-8.975E-05
4	-1.630E+05	-7.555E+05	-8.132E+05	6.434E-05	-6.897E-05	-8.195E-05
5	9.046E+05	9.046E+05	-3.547E+04	1.001E-04	1.001E-04	-1.115E-04
6	-3.705E+03	-3.705E+03	-3.547E+04	1.001E-04	1.001E-04	-3.288E-04
8	4.618E+05	0	-4.179E+05	1.013E-04	-2.565E-06	-9.658E-05
9	-5.867E+05	-1.251E+06	1.371E+06	5.514E-05	-9.421E-05	-1.213E-04
10	0	-9.337E+05	-1.308E+06	1.308E-04	-7.932E-05	-1.635E-04
11	-9.085E+04	-2.962E+05	-6.034E+05	3.733E-05	-8.874E-06	-7.798E-05
12	-5.887E+05	-1.122E+06	-1.239E+06	3.985E-05	-8.034E-05	-1.067E-04
13	-2.154E+05	-9.076E+05	-1.350E+06	9.578E-05	-5.996E-05	-1.595E-04
14	9.046E+05	9.046E+05	-3.547E+04	1.001E-04	1.001E-04	-1.115E-04
15	-3.694E+03	-3.705E+03	-3.548E+04	1.002E-04	1.002E-04	-3.289E-04

Table 6: Results of the example problems in terms of principal stresses and strains.

On sheets nr 1 and nr 7 of figure 49, we recognize the input. Please note on sheet 7 that the angle of the shear load is taken from the x-axis. Since the horizontal load is acting in the positive x-direction the shear direction equals 0^0 (the angle equals 180^0 if the shear load is acting in the negative x-direction). If the shear force was acting in the positive y-direction, the shear direction had to be 90^0. The sheets with the calculation results are pretty much self explaining. The coordinates of the location at which the stresses and strains are requested are given in the top of the page.

Then detailed information is given on the normal stresses and strains acting in the XX, YY and ZZ direction as well as on the shear stresses and strains in the YZ, XZ, and XY direction. All this information is summarized in terms of principal stresses and strains as well as the directions in which these principal stresses and strains are acting.

In table 6 a summary is given of these principal stresses and strains. When the results of sheet 5 (vertical load, bottom of the asphalt layer) are compared with those of sheet 14 (vertical load + shear load, bottom of the asphalt layer), we observe that those are exactly the same. This implies that the effect of the shear force is not "visible" at a depth of 250 mm. The same is true if we compare the results of sheets 6 and 15. The effect of the shear force is clearly visible when the results of sheet 3 (vertical load, location just outside loaded area at pavement surface) are compared with those obtained of sheets 8 and 9 (vertical load + shear load, location just outside loaded area at pavement surface).

In case of only a vertical load, σ_{xx} = -0.423 MPa (sheet 3). In case of a vertical and a horizontal load σ_{xx} = - 1.308 MPa (sheet 10) or σ_{xx} = 0.462 MPa (sheet 8). As one will observe, the applied braking force results in significant compressive horizontal stresses in front of the load in the direction of travel (x-direction) and a significant tensile stress at the back of the load. The principal strain at the pavement surface just behind the braking load (sheet 8) is slightly larger than the principal strain at the bottom of the asphalt layer (both are acting in the XX direction). Comparison of the results given in sheet 8 with those given in sheet 11 and comparison of the results given in sheet 10 with those given in sheet 13 show how the stresses and strains decrease with depth.

From this analysis it becomes clear that proper modeling of the contact stresses is very important in order to be able to analyze surface defects.

BISAR 3.0 - Detailed Report

(untitled)

System 1: (untitled)

Layer Number	Thickness (m)	Young's Modulus (Pa)	Poisson's Ratio	Shear Spring Compliance (m³/N)
1	0,250	6,000E+09	0,35	0,000E+00
2		1,000E+08	0,35	

1.

Load Number	Normal Stress (Pa)	Shear Stress (Pa)	Radius of Loaded Area (m)	Load - Position X (m)	Load - Position Y (m)	Shear Direction (°)
1	7,074E+05	0,000E+00	1,500E-01	0,000E+00	0,000E+00	0,000E+00

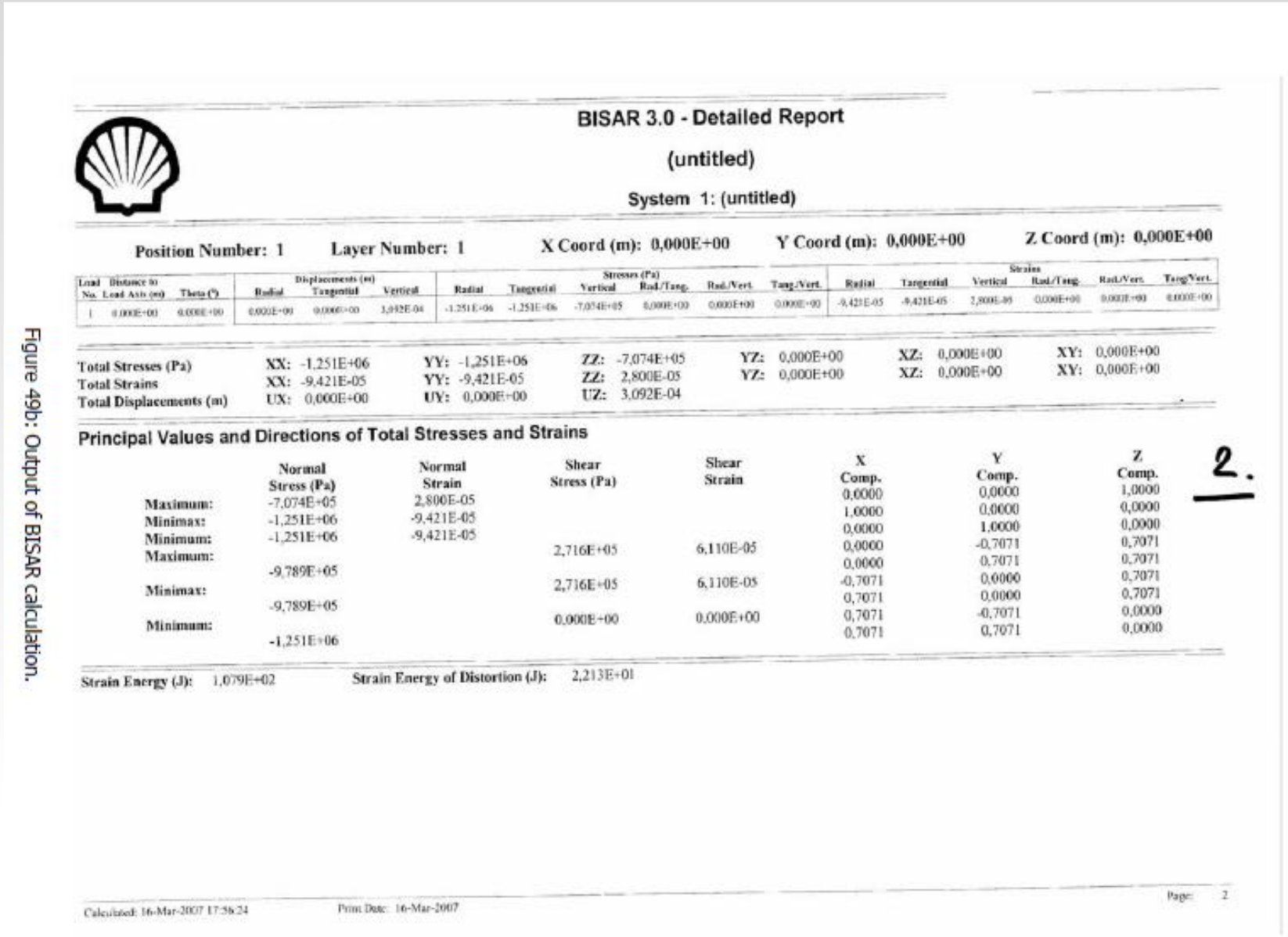

BISAR 3.0 - Detailed Report

(untitled)

System 1: (untitled)

Position Number: 1 **Layer Number: 1** **X Coord (m): 0,000E+00** **Y Coord (m): 0,000E+00** **Z Coord (m): 0,000E+00**

Load No.	Distance to Load Axis (m)	Theta (°)	Displacements (m) Radial	Tangential	Vertical	Stresses (Pa) Radial	Tangential	Vertical	Rad./Tang.	Rad./Vert.	Tang./Vert.	Strains Radial	Tangential	Vertical	Rad./Tang.	Rad./Vert.	Tang/Vert.
1	0,000E+00	0,000E+00	0,000E+00	0,000E+00	3,092E-04	-1,251E+06	-1,251E+06	-7,074E+05	0,000E+00	0,000E+00	0,000E+00	-9,421E-05	-9,421E-05	2,800E-05	0,000E+00	0,000E+00	0,000E+00

Total Stresses (Pa)	XX: -1,251E+06	YY: -1,251E+06	ZZ: -7,074E+05	YZ: 0,000E+00	XZ: 0,000E+00	XY: 0,000E+00
Total Strains	XX: -9,421E-05	YY: -9,421E-05	ZZ: 2,800E-05	YZ: 0,000E+00	XZ: 0,000E+00	XY: 0,000E+00
Total Displacements (m)	UX: 0,000E+00	UY: 0,000E+00	UZ: 3,092E-04			

Principal Values and Directions of Total Stresses and Strains

	Normal Stress (Pa)	Normal Strain	Shear Stress (Pa)	Shear Strain	X Comp.	Y Comp.	Z Comp.
Maximum:	-7,074E+05	2,800E-05			0,0000	0,0000	1,0000
Minimax:	-1,251E+06	-9,421E-05			1,0000	0,0000	0,0000
Minimum:	-1,251E+06	-9,421E-05			0,0000	1,0000	0,0000
Maximum:	-9,789E+05		2,716E+05	6,110E-05	0,0000	-0,7071	0,7071
					0,0000	0,7071	0,7071
Minimax:	-9,789E+05		2,716E+05	6,110E-05	-0,7071	0,0000	0,7071
					0,7071	0,0000	0,7071
Minimum:	-1,251E+06		0,000E+00	0,000E+00	0,7071	-0,7071	0,0000
					0,7071	0,7071	0,0000

Strain Energy (J): 1,079E+02 **Strain Energy of Distortion (J):** 2,213E+01

Calculated: 16-Mar-2007 17:56:24 Print Date: 16-Mar-2007 Page: 2

2.

Figure 49b: Output of BISAR calculation.

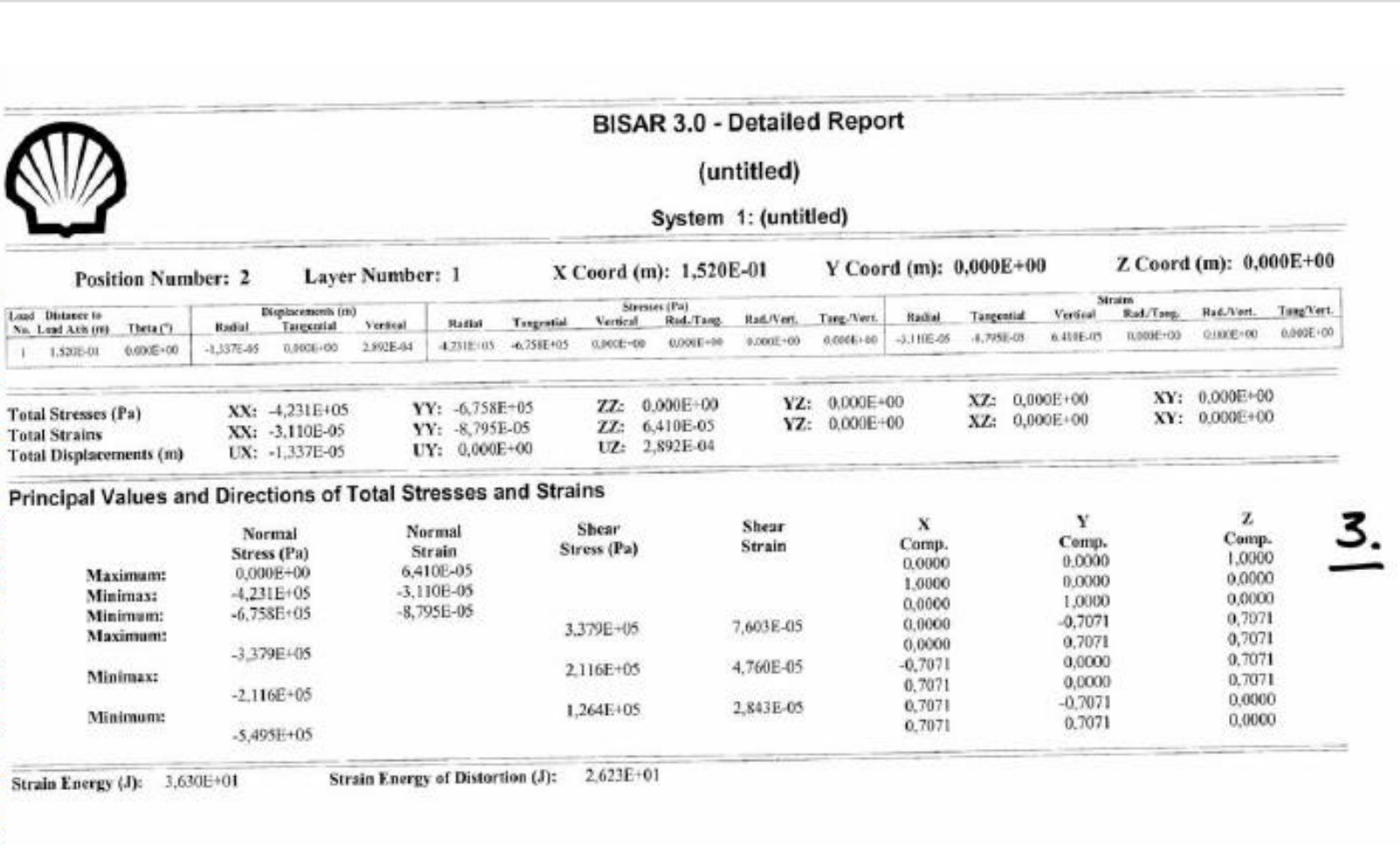

BISAR 3.0 - Detailed Report

(untitled)

System 1: (untitled)

Position Number: 2 Layer Number: 1 X Coord (m): 1,520E-01 Y Coord (m): 0,000E+00 Z Coord (m): 0,000E+00

Load No.	Distance to Load A(ft) (m)	Theta (°)	Displacements (m) Radial	Tangential	Vertical	Stresses (Pa) Radial	Tangential	Vertical	Rad./Tang.	Rad./Vert.	Tang./Vert.	Strains Radial	Tangential	Vertical	Rad./Tang.	Rad./Vert.	Tang/Vert.
1	1,520E-01	0,000E+00	-1,337E-05	0,000E+00	2,892E-04	-4,231E+05	-6,758E+05	0,000E+00	0,000E+00	0,000E+00	0,000E+00	-3,110E-05	-8,795E-05	6,410E-05	0,000E+00	0,000E+00	0,000E+00

Total Stresses (Pa)	XX: -4,231E+05	YY: -6,758E+05	ZZ: 0,000E+00	YZ: 0,000E+00	XZ: 0,000E+00	XY: 0,000E+00
Total Strains	XX: -3,110E-05	YY: -8,795E-05	ZZ: 6,410E-05	YZ: 0,000E+00	XZ: 0,000E+00	XY: 0,000E+00
Total Displacements (m)	UX: -1,337E-05	UY: 0,000E+00	UZ: 2,892E-04			

Principal Values and Directions of Total Stresses and Strains

	Normal Stress (Pa)	Normal Strain	Shear Stress (Pa)	Shear Strain	X Comp.	Y Comp.	Z Comp.
Maximum:	0,000E+00	6,410E-05			0,0000	0,0000	1,0000
Minimax:	-4,231E+05	-3,110E-05			1,0000	0,0000	0,0000
Minimum:	-6,758E+05	-8,795E-05			0,0000	1,0000	0,0000
Maximum:	-3,379E+05		3,379E+05	7,603E-05	0,0000	-0,7071	0,7071
Minimax:	-2,116E+05		2,116E+05	4,760E-05	0,0000	0,7071	0,7071
Minimum:	-5,495E+05		1,264E+05	2,843E-05	-0,7071	0,0000	0,7071
					0,7071	0,0000	0,0000
					0,7071	-0,7071	0,0000
					0,7071	0,7071	0,0000

Strain Energy (J): 3,630E+01 Strain Energy of Distortion (J): 2,623E+01

Calculated: 16-Mar-2007 17:56:24 Print Date: 16-Mar-2007 Page: 3

3.1

Figure 49 C: Output of BISAR calculation (continued).

BISAR 3.0 - Detailed Report

(untitled)

System 1: (untitled)

Position Number: 3 **Layer Number: 1** **X Coord (m): 1,520E-01** **Y Coord (m): 0,000E+00** **Z Coord (m): 1,000E-02**

Load No.	Distance to Load Axis (m)	Theta (°)	Displacements (m) Radial	Tangential	Vertical	Stresses (Pa) Radial	Tangential	Vertical	Rad./Tang.	Rad./Vert.	Tang./Vert.	Strains Radial	Tangential	Vertical	Rad./Tang.	Rad./Vert.	Tang./Vert.
1	1,520E-01	0,000E+00	-1,048E-05	0,000E+00	2,898E-04	-7,182E+05	-7,555E+05	-2,580E+05	0,000E+00	2,296E+05	0,000E+00	-6,058E-05	-6,897E-05	4,297E-05	0,000E+00	-5,167E-05	0,000E+00

Total Stresses (Pa)	**XX:** -7,182E+05	**YY:** -7,555E+05	**ZZ:** -2,580E+05	**YZ:** 0,000E+00	**XZ:** -2,296E+05	**XY:** 0,000E+00
Total Strains	**XX:** -6,058E-05	**YY:** -6,897E-05	**ZZ:** 4,297E-05	**YZ:** 0,000E+00	**XZ:** -5,167E-05	**XY:** 0,000E+00
Total Displacements (m)	**UX:** -1,048E-05	**UY:** 0,000E+00	**UZ:** 2,898E-04			

Principal Values and Directions of Total Stresses and Strains

	Normal Stress (Pa)	Normal Strain	Shear Stress (Pa)	Shear Strain	X Comp.	Y Comp.	Z Comp.
Maximum:	-1,630E+05	6,434E-05			-0,3822	0,0000	0,9241
Minimax:	-7,555E+05	-6,897E-05			0,0000	1,0000	0,0000
Minimum:	-8,132E+05	-8,195E-05			0,9241	0,0000	0,3822
Maximum:			3,251E+05	7,315E-05	-0,9237	0,0000	0,3832
	-4,881E+05				0,3832	0,0000	0,9237
Minimax:			2,962E+05	6,666E-05	-0,2703	-0,7071	0,6534
	-4,592E+05				-0,2703	0,7071	0,6534
Minimum:			2,885E+04	6,490E-06	-0,6534	0,7071	-0,2703
	-7,843E+05				0,6534	0,7071	0,2703

Strain Energy (J): 5,413E+01 **Strain Energy of Distortion (J):** 2,914E+01

Calculated: 16-Mar-2007 17:56:24 Print Date: 16-Mar-2007 Page 4

4.

Figure 49d: Output of BISAR calculation (continued).

BISAR 3.0 - Detailed Report

(untitled)

System 1: (untitled)

Position Number: 4 **Layer Number: 1** **X Coord (m): 0,000E+00** **Y Coord (m): 0,000E+00** **Z Coord (m): 2,500E-01**

Load No.	Distance to Load Axis (m)	Theta (°)	Displacements (m) Radial	Tangential	Vertical	Stresses (Pa) Radial	Tangential	Vertical	Rad./Tang.	Rad./Vert.	Tang./Vert.	Strains Radial	Tangential	Vertical	Rad./Tang.	Rad./Vert.	Tang/Vert.
1	0,000E+00	0,000E+00	0,000E+00	0,000E+00	2,957E-04	9,046E+05	9,046E+05	-3,547E+04	0,000E+00	0,000E+00	0,000E+00	1,001E-04	1,001E-04	-1,115E-04	0,000E+00	0,000E+00	0,000E+00

Total Stresses (Pa)	**XX:** 9,046E+05	**YY:** 9,046E+05	**ZZ:** -3,547E+04	**YZ:** 0,000E+00	**XZ:** 0,000E+00	**XY:** 0,000E+00
Total Strains	**XX:** 1,001E-04	**YY:** 1,001E-04	**ZZ:** -1,115E-04	**YZ:** 0,000E+00	**XZ:** 0,000E+00	**XY:** 0,000E+00
Total Displacements (m)	**UX:** 0,000E+00	**UY:** 0,000E+00	**UZ:** 2,957E-04			

Principal Values and Directions of Total Stresses and Strains

	Normal Stress (Pa)	Normal Strain	Shear Stress (Pa)	Shear Strain	X Comp.	Y Comp.	Z Comp.
Maximum:	9,046E+05	1,001E-04			1,0000	0,0000	0,0000
Minimax:	9,046E+05	1,001E-04			0,0000	1,0000	0,0000
Minimum:	-3,547E+04	-1,115E-04			0,0000	0,0000	1,0000
Maximum:			4,701E+05	1,058E-04	0,7071	0,0000	-0,7071
	4,346E+05				0,7071	0,0000	0,7071
Minimax:			4,701E+05	1,058E-04	0,0000	0,7071	-0,7071
	4,346E+05				0,0000	0,7071	0,7071
Minimum:			0,000E+00	0,000E+00	0,7071	-0,7071	0,0000
	9,046E+05				0,7071	0,7071	0,0000

Strain Energy (J): 9,251E+01 **Strain Energy of Distortion (J):** 6,629E+01

Calculated: 16-Mar-2007 17:56:24 Print Date: 16-Mar-2007 Page: 5

5.

Figure 49e: Output of BISAR calculation (continued).

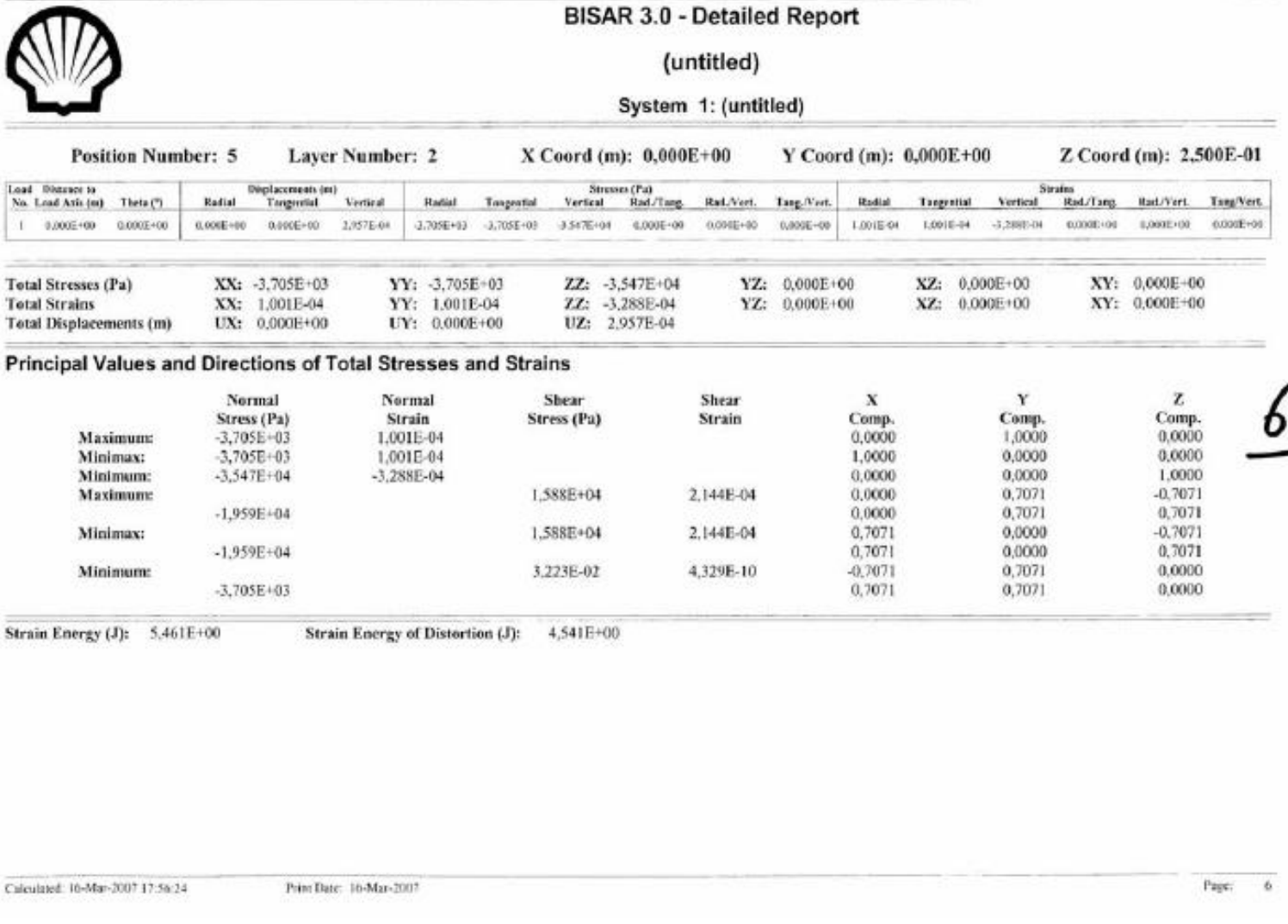

BISAR 3.0 - Detailed Report

(untitled)

System 1: (untitled)

Position Number: 5 **Layer Number: 2** **X Coord (m): 0,000E+00** **Y Coord (m): 0,000E+00** **Z Coord (m): 2,500E-01**

Load No.	Distance to Load Axis (m)	Theta (°)	Displacements (m) Radial	Tangential	Vertical	Stresses (Pa) Radial	Tangential	Vertical	Rad./Tang.	Rad./Vert.	Tang./Vert.	Strains Radial	Tangential	Vertical	Rad./Tang.	Rad./Vert.	Tang/Vert.
1	0,000E+00	0,000E+00	0,000E+00	0,000E+00	2,957E-04	-3,705E+03	-3,705E+03	-3,547E+04	0,000E+00	0,000E+00	0,000E+00	1,001E-04	1,001E-04	-3,288E-04	0,000E+00	0,000E+00	0,000E+00

Total Stresses (Pa)	**XX:** -3,705E+03	**YY:** -3,705E+03	**ZZ:** -3,547E+04	**YZ:** 0,000E+00	**XZ:** 0,000E+00	**XY:** 0,000E+00
Total Strains	**XX:** 1,001E-04	**YY:** 1,001E-04	**ZZ:** -3,288E-04	**YZ:** 0,000E+00	**XZ:** 0,000E+00	**XY:** 0,000E+00
Total Displacements (m)	**UX:** 0,000E+00	**UY:** 0,000E+00	**UZ:** 2,957E-04			

Principal Values and Directions of Total Stresses and Strains

	Normal Stress (Pa)	Normal Strain	Shear Stress (Pa)	Shear Strain	X Comp.	Y Comp.	Z Comp.
Maximum:	-3,705E+03	1,001E-04			0,0000	1,0000	0,0000
Minimax:	-3,705E+03	1,001E-04			1,0000	0,0000	0,0000
Minimum:	-3,547E+04	-3,288E-04			0,0000	0,0000	1,0000
Maximum:			1,588E+04	2,144E-04	0,0000	0,7071	-0,7071
	-1,959E+04				0,0000	0,7071	0,7071
Minimax:			1,588E+04	2,144E-04	0,7071	0,0000	-0,7071
	-1,959E+04				0,7071	0,0000	0,7071
Minimum:			3,223E-02	4,329E-10	-0,7071	0,7071	0,0000
	-3,705E+03				0,7071	0,7071	0,0000

Strain Energy (J): 5,461E+00 **Strain Energy of Distortion (J):** 4,541E+00

Calculated: 10-Mar-2007 17:56:24 Print Date: 10-Mar-2007 Page: 6

6.

Figure 49f: Output of BISAR calculation (continued).

BISAR 3.0 - Detailed Report

(untitled)

System 1: (untitled)

Layer Number	Thickness (m)	Young's Modulus (Pa)	Poisson's Ratio	Shear Spring Compliance (m³/N)
1	0,250	6,000E+09	0,35	0,000E+00
2		1,000E+08	0,35	

7.

Load Number	Normal Stress (Pa)	Shear Stress (Pa)	Radius of Loaded Area (m)	Load - Position X (m)	Load - Position Y (m)	Shear Direction (°)
1	7,074E+05	2,829E+05	1,500E-01	0,000E+00	0,000E+00	0,000E+00

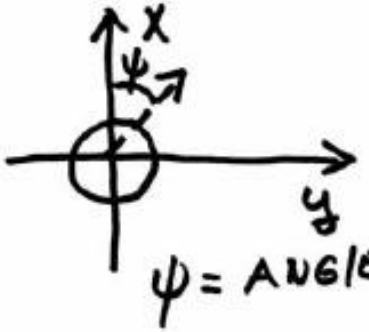

20 kN HORIZONTAL LOAD

ψ = ANGLE OF SHEAR DIRECTION

Calculated: 16-Mar-2007 17:49:37 Print Date: 16-Mar-2007 Page: 1

Figure 49g: Input for BISAR calculation; vertical and shear load.

BISAR 3.0 - Detailed Report

(untitled)

System 1: (untitled)

Position Number: 1 **Layer Number: 1** **X Coord (m): -1,520E-01** **Y Coord (m): 0,000E+00** **Z Coord (m): 0,000E+00**

Load No.	Distance to Load Axis (m)	Theta (°)	Displacements (m) Radial	Tangential	Vertical	Stresses (Pa) Radial	Tangential	Vertical	Rad./Tang.	Rad./Vert.	Tang./Vert.	Strains Radial	Tangential	Vertical	Rad./Tang.	Rad./Vert.	Tang/Vert.
1	1,520E-01	1,800E+02	-3,901E-05	2,127E-12	2,839E-04	4,618E+05	-4,179E+05	0,000E+00	3,354E-03	0,000E+00	0,000E+00	1,013E-04	-9,658E-05	-2,565E-06	7,546E-13	0,000E+00	0,000E+00

Total Stresses (Pa)	XX: 4,618E+05	YY: -4,179E+05	ZZ: 0,000E+00	YZ: 0,000E+00	XZ: 0,000E+00	XY: 3,354E-03
Total Strains	XX: 1,013E-04	YY: -9,658E-05	ZZ: -2,565E-06	YZ: 0,000E+00	XZ: 0,000E+00	XY: 7,546E-13
Total Displacements (m)	UX: 3,901E-05	UY: -2,127E-12	UZ: 2,839E-04			

Principal Values and Directions of Total Stresses and Strains

	Normal Stress (Pa)	Normal Strain	Shear Stress (Pa)	Shear Strain	X Comp.	Y Comp.	Z Comp.
Maximum:	4,618E+05	1,013E-04			1,0000	0,0000	0,0000
Minimax:	0,000E+00	-2,565E-06			0,0000	0,0000	1,0000
Minimum:	-4,179E+05	-9,658E-05			0,0000	1,0000	0,0000
Maximum:			4,398E+05	9,897E-05	0,7071	-0,7071	0,0000
	2,198E+04				0,7071	0,7071	0,0000
Minimax:			2,309E+05	5,196E-05	0,7071	0,0000	-0,7071
	2,309E+05				0,7071	0,0000	0,7071
Minimum:			2,089E+05	4,701E-05	0,0000	-0,7071	0,7071
	-2,089E+05				0,0000	0,7071	0,7071

Strain Energy (J): 4,358E+01 **Strain Energy of Distortion (J):** 4,357E+01

Calculated: 16-Mar-2007 17:49:37 Print Date: 16-Mar-2007 Page: 2

8.

Figure 49h: Output of BISAR calculation.

BISAR 3.0 - Detailed Report

(untitled)

System 1: (untitled)

Position Number: 2 **Layer Number: 1** **X Coord (m): 0,000E+00** **Y Coord (m): 0,000E+00** **Z Coord (m): 0,000E+00**

Load No.	Distance to Load Axis (m)	Theta (°)	Displacements (m) Radial	Tangential	Vertical	Stresses (Pa) Radial	Tangential	Vertical	Rad./Tang.	Rad./Vert.	Tang./Vert.	Strains Radial	Tangential	Vertical	Rad./Tang.	Rad./Vert.	Tang./Vert.
1	0,000E+00	0,000E+00	3,156E-05	0,000E+00	3,092E-04	-1,251E+06	-1,251E+06	-7,074E-05	0,000E+00	-2,829E+05	0,000E+00	-9,421E-05	-9,421E-05	2,800E-05	0,000E+00	-6,366E-05	0,000E+00

Total Stresses (Pa)	XX: -1,251E+06	YY: -1,251E+06	ZZ: -7,074E+05	YZ: 0,000E+00	XZ: -2,829E+05	XY: 0,000E+00
Total Strains	XX: -9,421E-05	YY: -9,421E-05	ZZ: 2,800E-05	YZ: 0,000E+00	XZ: -6,366E-05	XY: 0,000E+00
Total Displacements (m)	UX: 3,156E-05	UY: 0,000E+00	UZ: 3,092E-04			

Principal Values and Directions of Total Stresses and Strains

	Normal Stress (Pa)	Normal Strain	Shear Stress (Pa)	Shear Strain	X Comp.	Y Comp.	Z Comp.
Maximum:	-5,867E+05	5,514E-05			-0,3921	0,0000	0,9199
Minimax:	-1,251E+06	-9,421E-05			0,0000	1,0000	0,0000
Minimum:	-1,371E+06	-1,213E-04			0,9199	0,0000	0,3921
Maximum:			3,922E+05	8,824E-05	-0,9278	0,0000	0,3732
	-9,789E+05				0,3732	0,0000	0,9278
Minimax:			3,319E+05	7,467E-05	-0,2773	-0,7071	0,6505
	-9,186E+05				-0,2773	0,7071	0,6505
Minimum:			6,031E+04	1,357E-05	-0,6505	0,7071	-0,2773
	-1,311E+06				0,6505	0,7071	0,2773

Strain Energy (J): 1,259E+02 **Strain Energy of Distortion (J):** 4,014E+01

Calculated: 16-Mar-2007 17:49:17 Print Date: 16-Mar-2007 Page: 3

9.

Figure 49: Output of BISAR calculation (continued).

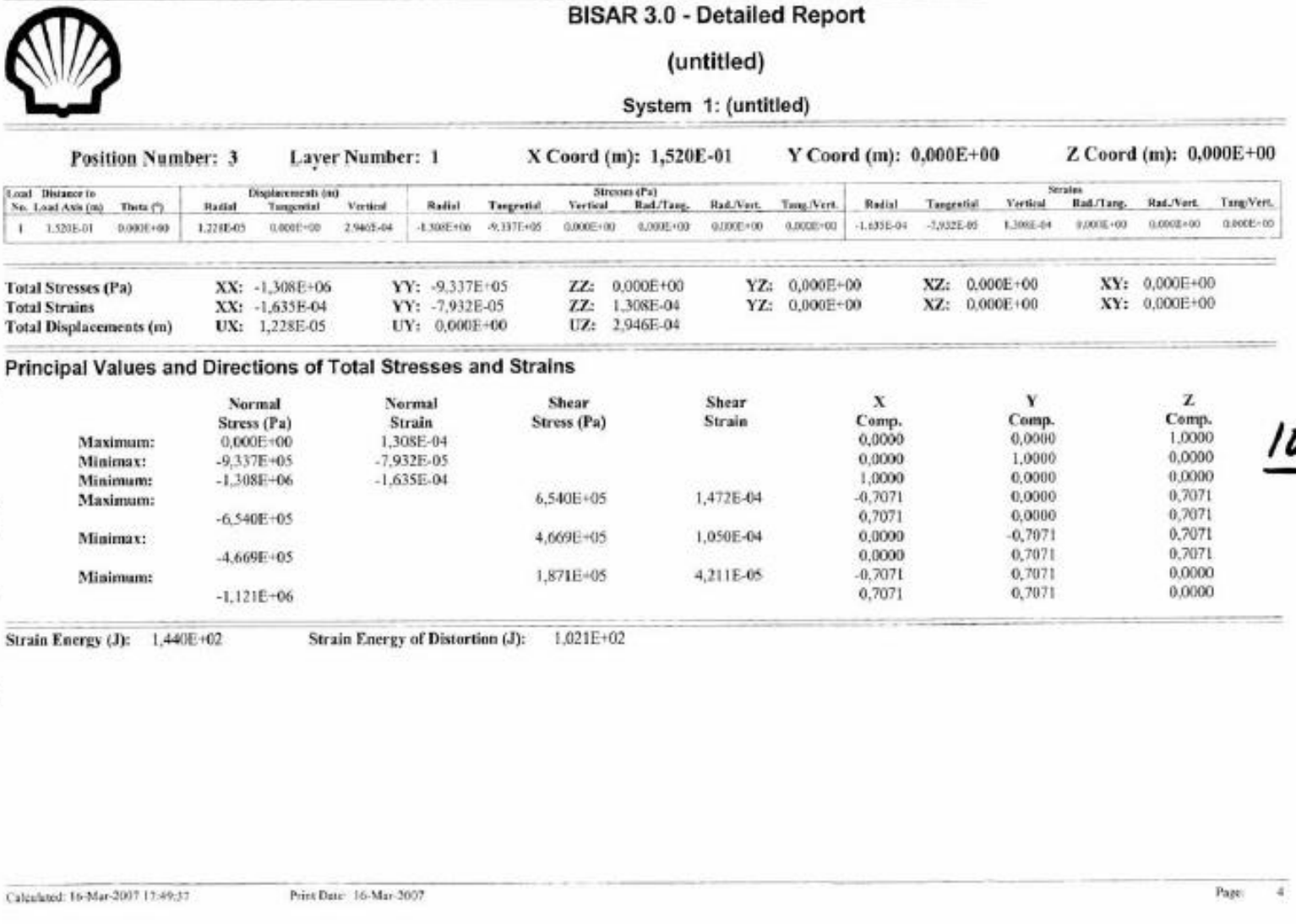

BISAR 3.0 - Detailed Report

(untitled)

System 1: (untitled)

Position Number: 3 **Layer Number: 1** **X Coord (m): 1,520E-01** **Y Coord (m): 0,000E+00** **Z Coord (m): 0,000E+00**

Load No.	Distance to Load Axis (m)	Theta (°)	Displacements (m) Radial	Tangential	Vertical	Stresses (Pa) Radial	Tangential	Vertical	Rad./Tang.	Rad./Vert.	Tang./Vert.	Strains Radial	Tangential	Vertical	Rad./Tang.	Rad./Vert.	Tang/Vert.
1	1,520E-01	0,000E+00	1,228E-05	0,000E+00	2,946E-04	-1,308E+06	-9,337E+05	0,000E+00	0,000E+00	0,000E+00	0,000E+00	-1,635E-04	-7,932E-05	1,308E-04	0,000E+00	0,000E+00	0,000E+00

Total Stresses (Pa)	**XX:** -1,308E+06	**YY:** -9,337E+05	**ZZ:** 0,000E+00	**YZ:** 0,000E+00	**XZ:** 0,000E+00	**XY:** 0,000E+00
Total Strains	**XX:** -1,635E-04	**YY:** -7,932E-05	**ZZ:** 1,308E-04	**YZ:** 0,000E+00	**XZ:** 0,000E+00	**XY:** 0,000E+00
Total Displacements (m)	**UX:** 1,228E-05	**UY:** 0,000E+00	**UZ:** 2,946E-04			

Principal Values and Directions of Total Stresses and Strains

	Normal Stress (Pa)	Normal Strain	Shear Stress (Pa)	Shear Strain	X Comp.	Y Comp.	Z Comp.
Maximum:	0,000E+00	1,308E-04			0,0000	0,0000	1,0000
Minimax:	-9,337E+05	-7,932E-05			0,0000	1,0000	0,0000
Minimum:	-1,308E+06	-1,635E-04			1,0000	0,0000	0,0000
Maximum:			6,540E+05	1,472E-04	-0,7071	0,0000	0,7071
	-6,540E+05				0,7071	0,0000	0,7071
Minimax:			4,669E+05	1,050E-04	0,0000	-0,7071	0,7071
	-4,669E+05				0,0000	0,7071	0,7071
Minimum:			1,871E+05	4,211E-05	-0,7071	0,7071	0,0000
	-1,121E+06				0,7071	0,7071	0,0000

Strain Energy (J): 1,440E+02 **Strain Energy of Distortion (J):** 1,021E+02

Calculated: 16-Mar-2007 17:49:37 Print Date: 16-Mar-2007 Page: 4

10.

Figure 49: Output of BISAR calculation (continued).

BISAR 3.0 - Detailed Report

(untitled)

System 1: (untitled)

Position Number: 4 **Layer Number: 1** **X Coord (m): -1,520E-01** **Y Coord (m): 0,000E+00** **Z Coord (m): 1,000E-02**

Load No.	Distance to Load Axis (m)	Theta (°)	Displacements (m) Radial	Tangential	Vertical	Stresses (Pa) Radial	Tangential	Vertical	Rad./Tang.	Rad./Vert.	Tang./Vert.	Strains Radial	Tangential	Vertical	Rad./Tang.	Rad./Vert.	Tang/Vert.
1	1,520E-01	1,800E+02	-3,548E-05	2,066E-12	2,841E-04	-2,144E+05	-6,034E+05	-1,727E+05	3,501E-03	-1,005E+05	1,706E-03	9,537E-06	-7,798E-05	1,892E-05	7,876E-13	-2,262E-05	3,838E-13

Total Stresses (Pa)	**XX:** -2,144E+05	**YY:** -6,034E+05	**ZZ:** -1,727E+05	**YZ:** -1,706E-03	**XZ:** 1,005E+05	**XY:** 3,501E-03
Total Strains	**XX:** 9,537E-06	**YY:** -7,798E-05	**ZZ:** 1,892E-05	**YZ:** -3,838E-13	**XZ:** 2,262E-05	**XY:** 7,876E-13
Total Displacements (m)	**UX:** 3,548E-05	**UY:** -2,066E-12	**UZ:** 2,841E-04			

Principal Values and Directions of Total Stresses and Strains

	Normal Stress (Pa)	Normal Strain	Shear Stress (Pa)	Shear Strain	X Comp.	Y Comp.	Z Comp.
Maximum:	-9,085E+04	3,733E-05			0,6312	0,0000	0,7756
Minimax:	-2,962E+05	-8,874E-06			0,7756	0,0000	-0,6312
Minimum:	-6,034E+05	-7,798E-05			0,0000	1,0000	0,0000
Maximum:			2,563E+05	5,766E-05	0,4463	-0,7071	0,5484
	-3,471E+05				0,4463	0,7071	0,5484
Minimax:			1,536E+05	3,455E-05	0,5484	-0,7071	-0,4463
	-4,498E+05				0,5484	0,7071	-0,4463
Minimum:			1,027E+05	2,310E-05	-0,1021	0,0000	0,9948
	-1,935E+05				0,9948	0,0000	0,1021

Strain Energy (J): 2,314E+01 **Strain Energy of Distortion (J):** 1,497E+01

Calculated: 16-Mar-2007 17:49:37 Print Date: 16-Mar-2007 Page 5

Figure 49k: Output of BISAR calculation (continued).

BISAR 3.0 - Detailed Report

(untitled)

System 1: (untitled)

Position Number: 5 **Layer Number: 1** **X Coord (m): 0,000E+00** **Y Coord (m): 0,000E+00** **Z Coord (m): 1,000E-02**

Load No.	Distance to Load Axis (m)	Theta (°)	Displacements (m) Radial	Tangential	Vertical	Stresses (Pa) Radial	Tangential	Vertical	Rad./Tang.	Rad./Vert.	Tang./Vert.	Strains Radial	Tangential	Vertical	Rad./Tang.	Rad./Vert.	Tang/Vert.
1	0,000E+00	0,000E+00	2,998E-05	0,000E+00	3,094E-04	-1,122E+06	-1,122E+06	-7,058E+05	0,000E+00	-2,498E+05	0,000E+00	-8,034E-05	-8,034E-05	1,323E-05	0,000E+00	-5,621E-05	0,000E+00

Total Stresses (Pa)	**XX:** -1,122E+06	**YY:** -1,122E+06	**ZZ:** -7,058E+05	**YZ:** 0,000E+00	**XZ:** -2,498E+05	**XY:** 0,000E+00
Total Strains	**XX:** -8,034E-05	**YY:** -8,034E-05	**ZZ:** 1,323E-05	**YZ:** 0,000E+00	**XZ:** -5,621E-05	**XY:** 0,000E+00
Total Displacements (m)	**UX:** 2,998E-05	**UY:** 0,000E+00	**UZ:** 3,094E-04			

Principal Values and Directions of Total Stresses and Strains

	Normal Stress (Pa)	Normal Strain	Shear Stress (Pa)	Shear Strain	X Comp.	Y Comp.	Z Comp.
Maximum:	-5,887E+05	3,958E-05			-0,4244	0,0000	0,9055
Minimax:	-1,122E+06	-8,034E-05			0,0000	1,0000	0,0000
Minimum:	-1,239E+06	-1,067E-04			0,9055	0,0000	0,4244
Maximum:			3,250E+05	7,313E-05	-0,9404	0,0000	0,3402
	-9,137E+05				0,3402	0,0000	0,9404
Minimax:			2,665E+05	5,996E-05	-0,3001	-0,7071	0,6403
	-8,552E+05				-0,3001	0,7071	0,6403
Minimum:			5,854E+04	1,317E-05	-0,6403	0,7071	-0,3001
	-1,180E+06				0,6403	0,7071	0,3001

Strain Energy (J): 9,949E+01 **Strain Energy of Distortion (J):** 2,701E+01

Calculated: 16-Mar-2007 17:49:37 Print Date: 16-Mar-2007 Page: 6

12.

Figure 49l: Output of BISAR calculation (continued).

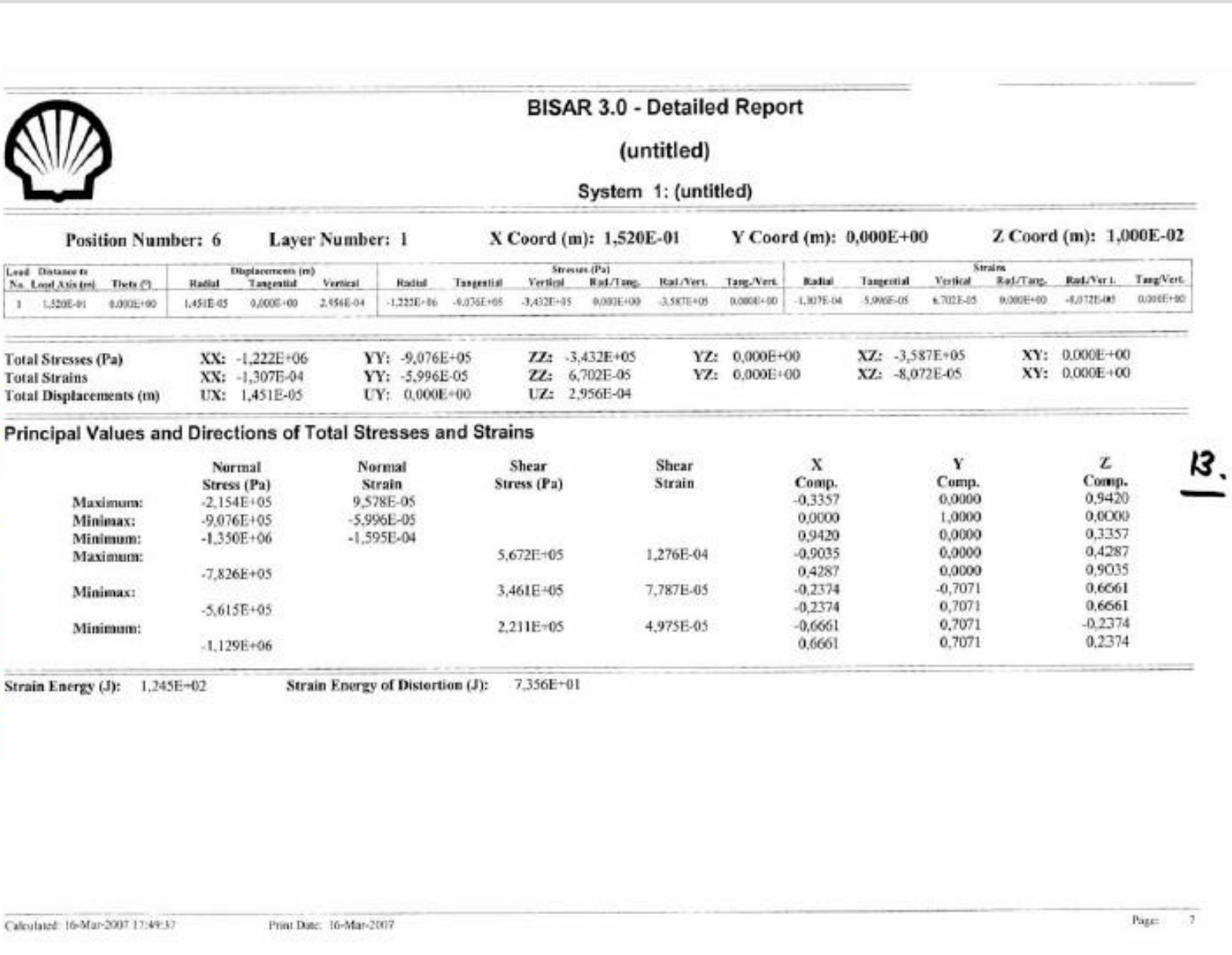

BISAR 3.0 - Detailed Report

(untitled)

System 1: (untitled)

Position Number: 6 **Layer Number: 1** **X Coord (m): 1,520E-01** **Y Coord (m): 0,000E+00** **Z Coord (m): 1,000E-02**

Load No.	Distance to Load Axis (m)	Theta (°)	Displacements (m) Radial	Tangential	Vertical	Stresses (Pa) Radial	Tangential	Vertical	Rad./Tang.	Rad./Vert.	Tang./Vert.	Strains Radial	Tangential	Vertical	Rad./Tang.	Rad./Vert.	Tang/Vert.
1	1,520E-01	0,000E+00	1,451E-05	0,000E+00	2,956E-04	-1,222E+06	-9,076E+05	-3,432E+05	0,000E+00	-3,587E+05	0,000E+00	-1,307E-04	-5,996E-05	6,702E-05	0,000E+00	-8,072E-05	0,000E+00

Total Stresses (Pa)	**XX:** -1,222E+06	**YY:** -9,076E+05	**ZZ:** -3,432E+05	**YZ:** 0,000E+00	**XZ:** -3,587E+05	**XY:** 0,000E+00
Total Strains	**XX:** -1,307E-04	**YY:** -5,996E-05	**ZZ:** 6,702E-05	**YZ:** 0,000E+00	**XZ:** -8,072E-05	**XY:** 0,000E+00
Total Displacements (m)	**UX:** 1,451E-05	**UY:** 0,000E+00	**UZ:** 2,956E-04			

Principal Values and Directions of Total Stresses and Strains

	Normal Stress (Pa)	Normal Strain	Shear Stress (Pa)	Shear Strain	X Comp.	Y Comp.	Z Comp.
Maximum:	-2,154E+05	9,578E-05			-0,3357	0,0000	0,9420
Minimax:	-9,076E+05	-5,996E-05			0,0000	1,0000	0,0000
Minimum:	-1,350E+06	-1,595E-04			0,9420	0,0000	0,3357
Maximum:			5,672E+05	1,276E-04	-0,9035	0,0000	0,4287
	-7,826E+05				0,4287	0,0000	0,9035
Minimax:			3,461E+05	7,787E-05	-0,2374	-0,7071	0,6661
	-5,615E+05				-0,2374	0,7071	0,6661
Minimum:			2,211E+05	4,975E-05	-0,6661	0,7071	-0,2374
	-1,129E+06				0,6661	0,7071	0,2374

Strain Energy (J): 1,245E+02 **Strain Energy of Distortion (J):** 7,356E+01

Calculated: 16-Mar-2007 17:49:37 Print Date: 16-Mar-2007 Page: 7

13.

Figure 49m: Output of BISAR calculation (continued).

BISAR 3.0 - Detailed Report

(untitled)

System 1: (untitled)

Position Number: 7 **Layer Number: 1** **X Coord (m): 0,000E+00** **Y Coord (m): 0,000E+00** **Z Coord (m): 2,500E-01**

Load No.	Distance to Load Axis (m)	Theta (°)	Displacements (m) Radial	Tangential	Vertical	Stresses (Pa) Radial	Tangential	Vertical	Rad./Tang.	Rad./Vert.	Tang./Vert.	Strains Radial	Tangential	Vertical	Rad./Tang.	Rad./Vert.	Tang/Vert.
1	0.000E+00	0.00E+00	1.408E-05	0.00E+00	2.957E-04	9.046E+05	9.046E+05	-3.547E+04	0.000E+00	5.943E+02	0.000E+00	1.001E-04	1.001E-04	-1.115E-04	0.000E+00	1.337E-07	0.000E+00

Total Stresses (Pa)	XX: 9,046E+05	YY: 9,046E+05	ZZ: -3,547E+04	YZ: 0,000E+00	XZ: 5,943E+02	XY: 0,000E+00
Total Strains	XX: 1,001E-04	YY: 1,001E-04	ZZ: -1,115E-04	YZ: 0,000E+00	XZ: 1,337E-07	XY: 0,000E+00
Total Displacements (m)	UX: 1,408E-05	UY: 0,000E+00	UZ: 2,957E-04			

Principal Values and Directions of Total Stresses and Strains

	Normal Stress (Pa)	Normal Strain	Shear Stress (Pa)	Shear Strain	X Comp.	Y Comp.	Z Comp.
Maximum:	9,046E+05	1,001E-04			1,0000	0,0000	0,0006
Minimax:	9,046E+05	1,001E-04			0,0000	1,0000	0,0000
Minimum:	-3,547E+04	-1,115E-04			-0,0006	0,0000	1,0000
Maximum:			4,701E+05	1,058E-04	0,7076	0,0000	-0,7067
	4,346E+05				0,7067	0,0000	0,7076
Minimax:			4,701E+05	1,058E-04	0,0004	0,7071	-0,7071
	4,346E+05				-0,0004	0,7071	0,7071
Minimum:			1,875E-01	4,366E-11	0,7071	-0,7071	0,0004
	9,046E+05				0,7071	0,7071	0,0004

Strain Energy (J): 9,251E+01 **Strain Energy of Distortion (J):** 6,629E+01

Calculated: 16-Mar-2007 17:49:37 Print Date: 16-Mar-2007 Page: 8

14.

Figure 49n: Output of BISAR calculation (continued).

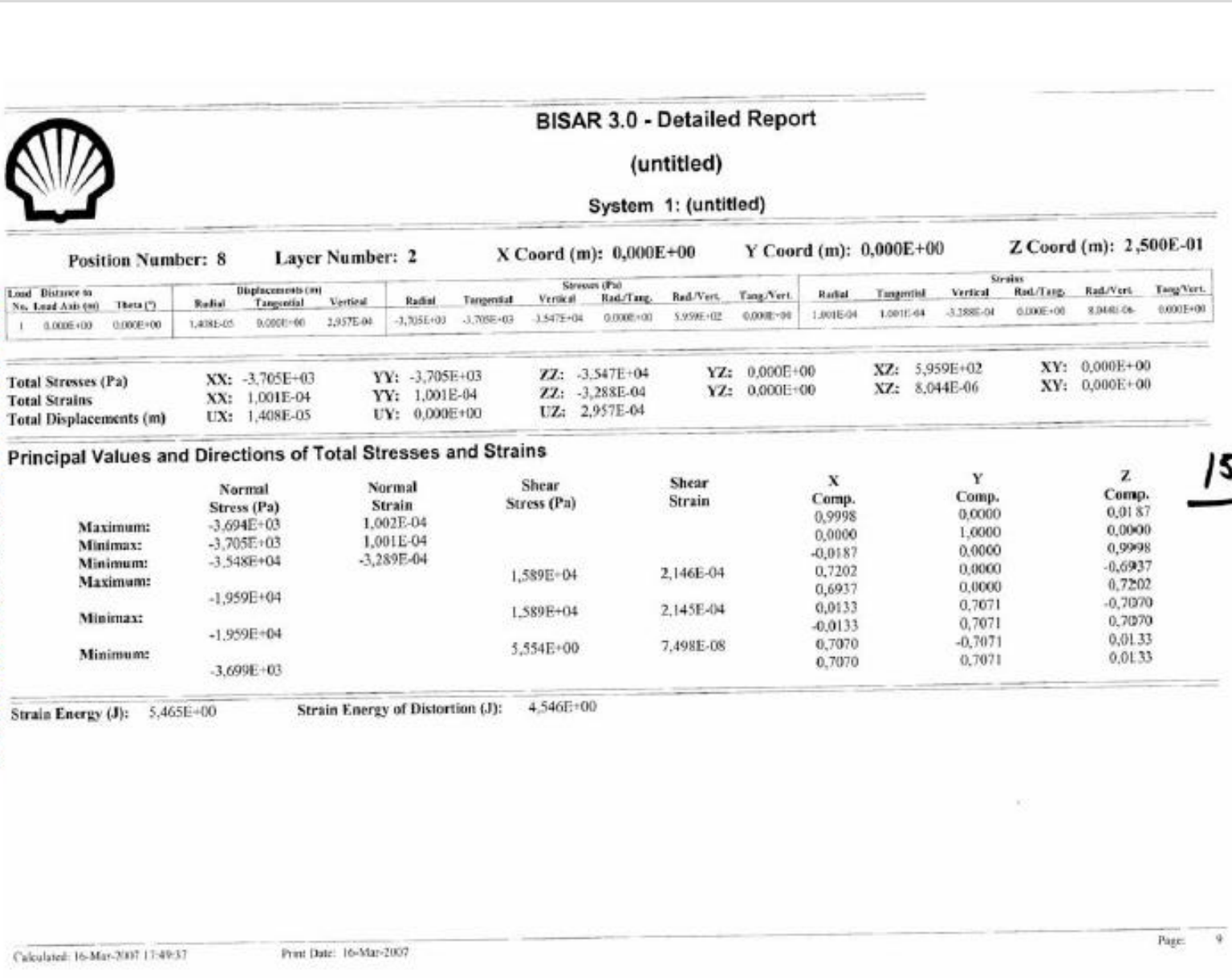

BISAR 3.0 - Detailed Report

(untitled)

System 1: (untitled)

Position Number: 8 Layer Number: 2 X Coord (m): 0,000E+00 Y Coord (m): 0,000E+00 Z Coord (m): 2,500E-01

Load No.	Distance to Load Axis (m)	Theta (°)	Displacements (m) Radial	Tangential	Vertical	Stresses (Pa) Radial	Tangential	Vertical	Rad./Tang.	Rad./Vert.	Tang./Vert.	Strains Radial	Tangential	Vertical	Rad./Tang.	Rad./Vert.	Tang./Vert.
1	0.000E+00	0.000E+00	1,408E-05	0,000E+00	2,957E-04	-3,705E+03	-3,705E+03	-3,547E+04	0,000E+00	5,959E+02	0,000E+00	1,001E-04	1,001E-04	-3,288E-04	0,000E+00	8,044E-06	0,000E+00

Total Stresses (Pa)	XX: -3,705E+03	YY: -3,705E+03	ZZ: -3,547E+04	YZ: 0,000E+00	XZ: 5,959E+02	XY: 0,000E+00
Total Strains	XX: 1,001E-04	YY: 1,001E-04	ZZ: -3,288E-04	YZ: 0,000E+00	XZ: 8,044E-06	XY: 0,000E+00
Total Displacements (m)	UX: 1,408E-05	UY: 0,000E+00	UZ: 2,957E-04			

Principal Values and Directions of Total Stresses and Strains

	Normal Stress (Pa)	Normal Strain	Shear Stress (Pa)	Shear Strain	X Comp.	Y Comp.	Z Comp.
Maximum:	-3,694E+03	1,002E-04			0,9998	0,0000	0,0187
Minimax:	-3,705E+03	1,001E-04			0,0000	1,0000	0,0000
Minimum:	-3,548E+04	-3,289E-04			-0,0187	0,0000	0,9998
Maximum:			1,589E+04	2,146E-04	0,7202	0,0000	-0,6937
	-1,959E+04				0,6937	0,0000	0,7202
Minimax:			1,589E+04	2,145E-04	0,0133	0,7071	-0,7070
	-1,959E+04				-0,0133	0,7071	0,7070
Minimum:			5,554E+00	7,498E-08	0,7070	-0,7071	0,0133
	-3,699E+03				0,7070	0,7071	0,0133

Strain Energy (J): 5,465E+00 Strain Energy of Distortion (J): 4,546E+00

Calculated: 16-Mar-2007 17:49:37 Print Date: 16-Mar-2007 Page: 9

15.

Figure 49o: Output of BISAR calculation (continued).